

200  
10-17-69

MLM-1659

1043

MLM-1659

SNAP-19B(IRHS) RECOVERED HEAT SOURCES  
FINAL REPORT

MASTER

D. E. Loyer and C. H. Davenport

AEC Research and Development REPORT

MONSANTO RESEARCH CORPORATION

A SUBSIDIARY OF MONSANTO COMPANY



M O U N D   L A B O R A T O R Y

MIAMISBURG, OHIO

OPERATED FOR

UNITED STATES ATOMIC ENERGY COMMISSION

U.S. GOVERNMENT CONTRACT NO. AT-33-1-GEN-53

## **DISCLAIMER**

**This report was prepared as an account of work sponsored by an agency of the United States Government. Neither the United States Government nor any agency Thereof, nor any of their employees, makes any warranty, express or implied, or assumes any legal liability or responsibility for the accuracy, completeness, or usefulness of any information, apparatus, product, or process disclosed, or represents that its use would not infringe privately owned rights. Reference herein to any specific commercial product, process, or service by trade name, trademark, manufacturer, or otherwise does not necessarily constitute or imply its endorsement, recommendation, or favoring by the United States Government or any agency thereof. The views and opinions of authors expressed herein do not necessarily state or reflect those of the United States Government or any agency thereof.**

## **DISCLAIMER**

**Portions of this document may be illegible in electronic image products. Images are produced from the best available original document.**

Printed in the United States of America  
Available from  
Clearinghouse for Federal Scientific and Technical Information  
National Bureau of Standards, U. S. Department of Commerce  
Springfield, Virginia 22151  
Price: Printed Copy \$3.00; Microfiche \$0.65

## LEGAL NOTICE

This report was prepared as an account of Government sponsored work. Neither the United States, nor the Commission, nor any person acting on behalf of the Commission:

- A. Makes any warranty or representation, expressed or implied, with respect to the accuracy, completeness, or usefulness of the information contained in this report, or that the use of any information, apparatus, method, or process disclosed in this report may not infringe privately owned rights; or
- B. Assumes any liabilities with respect to the use of, or for damages resulting from the use of any information, apparatus, method, or process disclosed in this report.

As used in the above, "person acting on behalf of the Commission" includes any employee or contractor of the Commission, or employee of such contractor, to the extent that such employee or contractor of the Commission, or employee of such contractor prepares, disseminates, or provides access to, any information pursuant to his employment or contract with the Commission, or his employment with such contractor.

MLM-1659  
TID-4500  
UC-23 Radioisotope  
and Radiation Applications

**SNAP-19B(IRHS) RECOVERED HEAT SOURCES  
FINAL REPORT**

D. E. Loyer  
C. H. Davenport

**Issued: September 15, 1969**

**MONSANTO RESEARCH CORPORATION**

A Subsidiary of Monsanto Company

**MOUND LABORATORY**

Miamisburg, Ohio

operated for

**UNITED STATES ATOMIC ENERGY COMMISSION**

U S. GOVERNMENT CONTRACT NO AT-33-1-GEN-53

**LEGAL NOTICE**

This report was prepared as an account of Government sponsored work. Neither the United States, nor the Commission, nor any person acting on behalf of the Commission:

A. Makes any warranty or representation, expressed or implied, with respect to the accuracy, completeness, or usefulness of the information contained in this report, or that the use of any information, apparatus, method, or process disclosed in this report may not infringe privately owned rights; or

B. Assumes any liabilities with respect to the use of, or for damages resulting from the use of any information, apparatus, method, or process disclosed in this report.

As used in the above, "person acting on behalf of the Commission" includes any employee or contractor of the Commission, or employee of such contractor, to the extent that such employee or contractor of the Commission, or employee of such contractor prepares, disseminates, or provides access to, any information pursuant to his employment or contract with the Commission, or his employment with such contractor.

## TABLE OF CONTENTS

	<u>Page</u>
I. SUMMARY . . . . .	8
II. INTRODUCTION . . . . .	9
III. DISASSEMBLY OF HEAT SOURCE SN 375/369	
A. Graphite Heat Shield . . . . .	9
B. Canister . . . . .	12
C. Capsule . . . . .	12
D. Fuel Removal . . . . .	15
E. General Comments . . . . .	18
IV. DISASSEMBLY OF HEAT SOURCE 361/368	
A. Graphite Heat Shield . . . . .	18
B. Canister . . . . .	22
C. Capsule. . . . .	23
D. Fuel Removal . . . . .	25
E. General Comments . . . . .	26
V. ACKNOWLEDGMENT. . . . .	27
VI. REFERENCES . . . . .	27
VII. APPENDICES	
A. Results of Characterization of Free-Flowing Fuel from Capsules 375/369 and 361/368 . . . . .	29
B. Summary of Fines Data from Capsules SN 375/369, 361/368 and 309. . . . .	33
C. Summary Report of Plutonium-238 Particulate Material Less than 10 $\mu\text{m}$ in Size as Removed from Free-Flowing Fuel Contained in Capsule 375/369 . . .	37

TABLE OF CONTENTS (continued)

	<u>Page</u>
D. Summary Report of Plutonium-238 Particulate Material Less than 10 $\mu\text{m}$ in Size as Removed from Historical Sample #309 . . . . .	45
E. Summary Report of Plutonium-238 Particulate Material Less than 10 $\mu\text{m}$ in Size as Removed from Free-Flowing Fuel Contained in Capsule 361/368 . . .	53

## ILLUSTRATIONS

<u>Photograph Number</u>	<u>Title</u>	<u>Page</u>
1	Heat Source 375/369 Without Heat Accumulator Block	10
2	Unscrewing the Graphite Block	10
3	Unscrewing the Graphite Block	10
4	Unscrewing the Graphite Block	11
5	Female Half of Heat Shield with Water Inside	11
6	Canistered Capsule Showing Deposits on Canistered Surface	11
7	Graphite Halves Showing the Cracked Areas	12
8	Canistered Capsule Completely Removed from Graphite Heat Shield	13
9	Canistered Capsule Showing Disintegrated Portion of Canister Sleeve	13
10	Canister Pieces	13
11	Vent End of Capsule	14
12	Canistered Capsule with Various Colored Deposits on Surface	14
13	Container for Storing the Heat Source after Disassembly	15
14	Fixturing Inside Box Used for Drilling the Capsule, Recording the Internal Pressure and Collecting a Gas Sample	15
15	Upper Portion of Capsule Exposing Fuel	17

ILLUSTRATIONS (continued)

<u>Photograph Number</u>	<u>Title</u>	<u>Page</u>
16	Removal of Agglomerated Fuel	17
17	Removal of Heat Accumulator Block from Heat Source SN 361/368	19
18	Heat Source SN 361/368 with Heat Accumulator Block Off	19
19	Heat Source SN 361/368 with Heat Accumulator Block Off (90° from Photograph 18)	20
20	Heat Source SN 361/368 with Heat Accumulator Block Off (180° from Photograph 18)	20
21	Use of Strap Wrenches to Unscrew the Graphite Block	20
22	Use of Strap Wrenches to Unscrew the Graphite Heat Block	20
23	Exposed Canistered Capsule with Tantalum Pad Stuck to Domed End	21
24	Exposed Canistered Capsule with Male Section of Graphite Heat Shield Broken Off	21
25	Exposed Canistered Capsule	21
26	Exposed Canistered Capsule	21
27	Exposed Canistered Capsule	22
28	Exposed Canistered Capsule	22
29	Exposed Canistered Capsule Showing Area that was Broken to Initiate Canister Sleeve Removal	22
30	Exposed Domed Vent End with Canister Cap Removed	23
31	Capsule Components After Removal	23
32	Graphite Heat Shield Section	24

ILLUSTRATIONS (continued)

<u>Photograph Number</u>	<u>Title</u>	<u>Page</u>
33	Capsule Showing Green Streaks	24
34	Capsule with Canister Removed	24
35	Elutriation Column Containing Plutonium-238 Microspheres	26
36	Capsule Vent End Lifted Up to Show Exposed Fuel	27
37	Capsule Vent End Removed to Show Exposed Fuel	27

## Tables

<u>Table Number</u>	<u>Title</u>	<u>Page</u>
1	Analysis of White Deposit from Vent End of Capsule SN 375/369	14
2	Analysis of Gas Released from Capsule SN 375/369	16
3	Calculated Internal Pressure Corresponding to Assumed Average Surface Temperature of Capsule SN 375/369	17

## FIGURES

<u>Figure Number</u>	<u>Title</u>	
1	Schematic Drawing of Internal Pressure Manifold	16
2	Schematic Drawing of Elutriation Wash Apparatus for Fines Determination	25

## I. SUMMARY

Two SNAP-19B (IRHS) heat sources which had fallen into the Pacific Ocean on May 18, 1968, as a result of the abort of a NIMBUS-B satellite were recovered on October 9, 1968, and returned to Mound Laboratory for examination and fuel recovery.

A health physics survey of the sources revealed no release of radioactivity. A set of procedures for extensive examination of the two capsules was prepared. The heat sources were radiographed and photographed in the as-received condition. The radiographs indicated that the fuel was agglomerated, but was still contained within the capsule.

Since the start of the examination on January 9, 1969, both heat sources were disassembled; the fuel was removed and fully characterized; fines analyses were conducted on free-flowing fuel from each capsule; heat source components were metallographically examined; and vents were flow-checked and metallographically examined.

The examination revealed that while the fuel sintered due to being exposed to high temperature for a prolonged period of time, no other changes in the fuel occurred.

## II. INTRODUCTION

On May 18, 1968, a NIMBUS-B weather satellite was launched from Vandenberg Air Force Base, California, but due to a malfunction had to be aborted approximately one minute after launch. The satellite carried two SNAP-19B nuclear generators developed under the program of the Atomic Energy Commission, Division of Space Nuclear Systems. Each generator contained a SNAP-19B Intact-Upon-Reentry Heat Source (IRHS) which was loaded with  $^{238}\text{PuO}_2$  fuel capable of furnishing  $\sim 575 \text{ W(t)}$ .

The satellite and generator debris was located in the Pacific Ocean on September 26, 1968, about 4 mi (6.4 km) north of San Miguel Island off the coast of California at a depth of about 325 ft (99.1 m). The two heat sources (SN 375/369 and SN 361/368) were recovered on October 9, 1968, and were delivered to Monsanto Research Corporation (MRC), Mound Laboratory, at Miamisburg, Ohio, on October 12, 1968, for fuel recovery and examination of capsules and fuel.

This was the first time that heat sources had been in an abort environment other than simulated laboratory conditions; they had also been exposed to sea water for 5 mo at  $\sim 20$  atm pressure. The procedures for the disassembly of the capsules and characterization of the fuel were established to determine the effect of the abort and sea water exposure.

Initially a health physics survey revealed that there had been no release of radioactivity. Radiographs indicated that the fuel was agglomerated, but was still contained within the capsule.

## III. DISASSEMBLY OF HEAT SOURCE SN 375/369

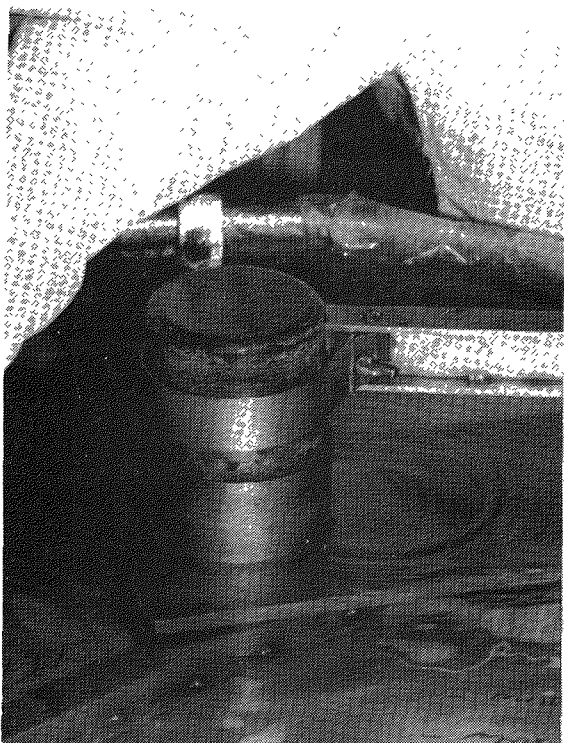
- A. The graphite heat shield was removed from heat source SN 375/369 on January 9, 1969. The heat shield did not have a heat accumulator block around it as was the case for source SN 361/368 (see Section IV of this report). The shield had a crack extending  $\sim 3$  in. (7.62 cm) along the thread area of the male half (Photograph 1). Also, a small crack extended about 1 in. (2.54 cm) at a  $45^\circ$  angle to the closure gap in the thread area of the female half. It was felt that this crack could have been caused by the anchor chain of the recovery vessel striking the source during the recovery operation. Overall dimensions were taken but due to the unevenness of the surface caused by deposits, it was difficult to obtain a meaningful comparison of these dimensions with those taken originally.



PHOTOGRAPH 1 - Heat source 375/369 without heat accumulator block.

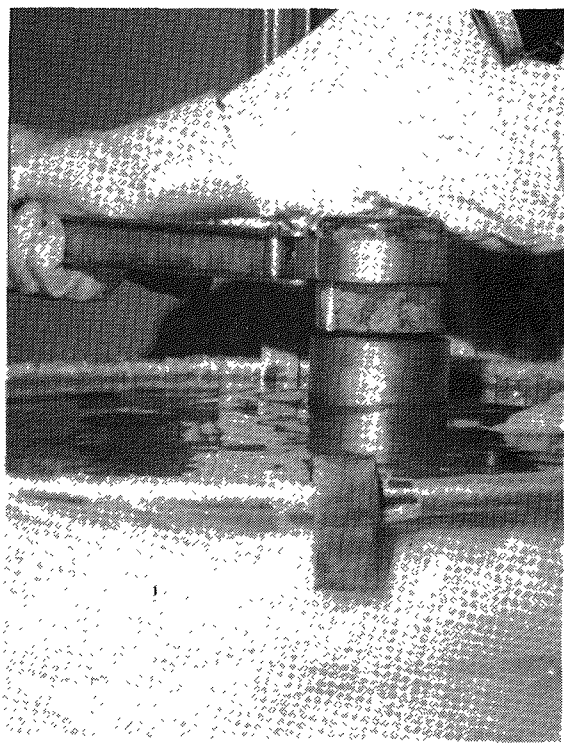
690097

Upon completion of a health physics survey which indicated no release of alpha contamination, the heat source was placed into a holder and a strap wrench was attached to each half of the graphite heat shield (Photographs 2, 3, 4). Initially, a small torque was needed to unscrew the graphite halves but after several turns, the unscrewing became easy. The same strap wrenches, holder, and personnel that were used in the original assembly in December, 1967, were employed for this disassembly operation. As the last few threads were approached,



PHOTOGRAPH 2 - Unscrewing the graphite block.

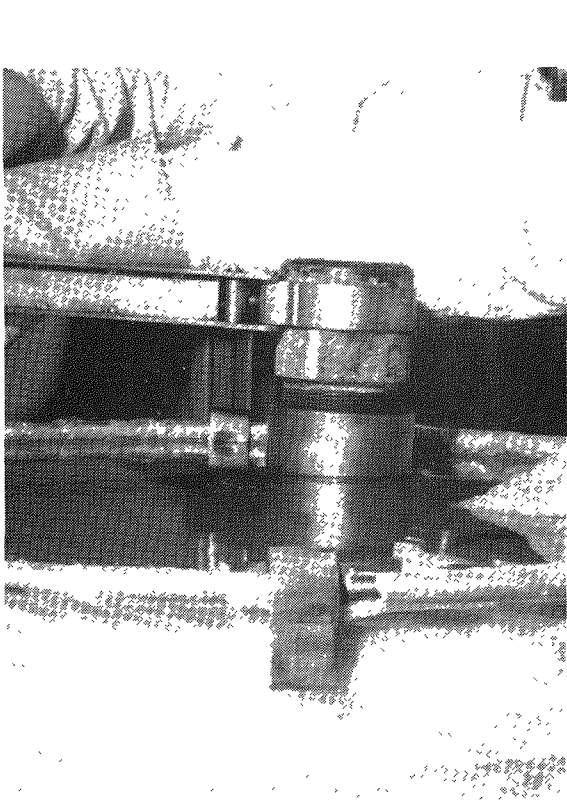
L - 690107 R - 690112



PHOTOGRAPH 3 - Unscrewing the graphite block.

L - 690109 R - 690108

690099



PHOTOGRAPH 4 - Unscrewing the graphite block.

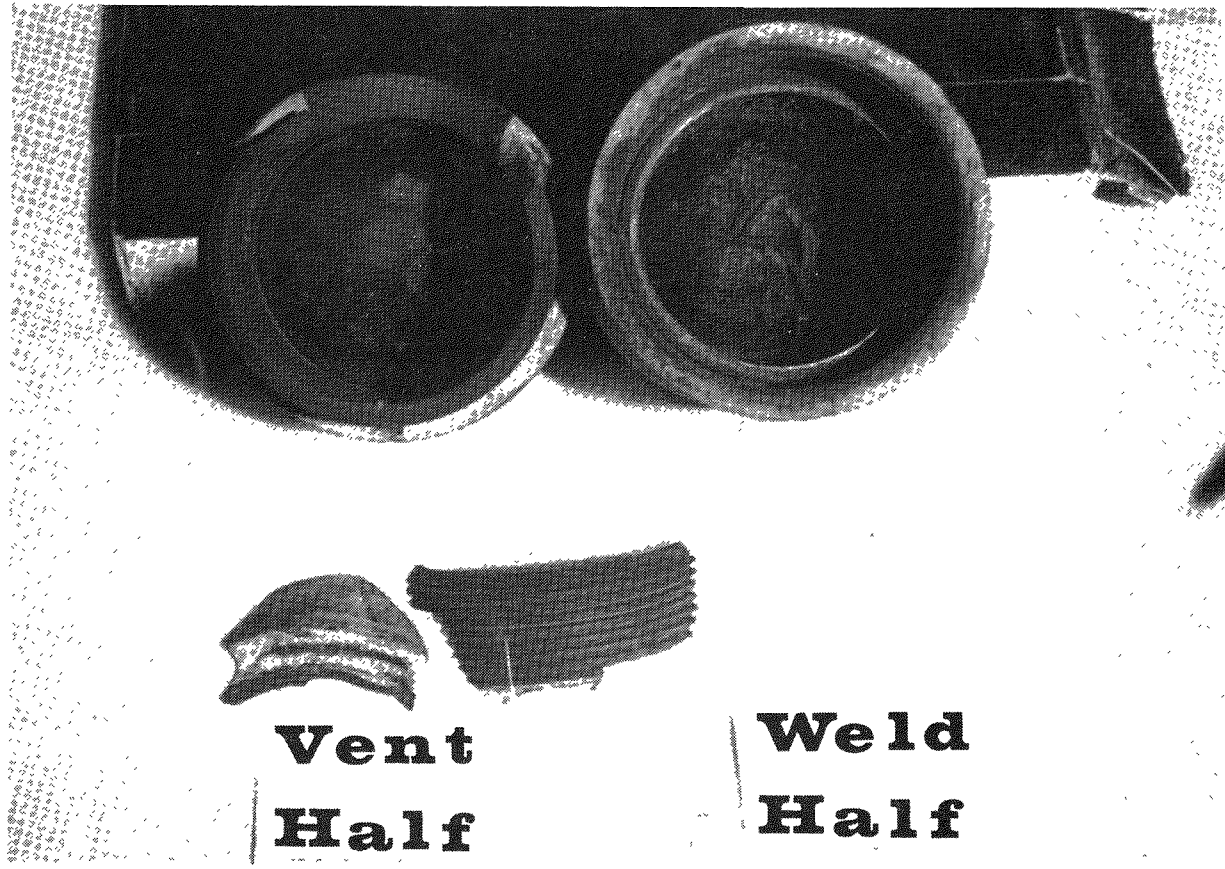


PHOTOGRAPH 5 - Female half of heat shield with water inside.

water began to come out from around the threads. The female half (fueling end) came off with ease, but there was some difficulty in removing the male half (vent end). Water was present inside the heat shield (Photograph 5), and deposits had built up between the canister and the internal graphite wall (Photograph 6). The internal ceramic coating on the graphite had come off in small chunks from the mid-section and had adhered to the area above the felt pads. The graphite pieces that were in the cracked area had broken out (male half) as can be seen in Photograph 7. The felt compliance pads were compressed and resembled burnt steel wool.



PHOTOGRAPH 6 - Canistered capsule showing deposits on canistered surface.



690106

PHOTOGRAPH 7 - Graphite halves showing the cracked areas.

B. Canister

The canistered capsule had salt deposits on its surface (Photograph 8). A portion of the canistered sleeve had disintegrated (Photograph 9). The canister cap was removed intact (Photograph 10); it had a small crack starting from the edge and ending just below the center of the cap. The canister was embrittled and parts broke while being disassembled (Photograph 10). The coatings on the inside of the canister had come off in several areas. The canister was submitted to metallurgy for inspection.

C. Capsule

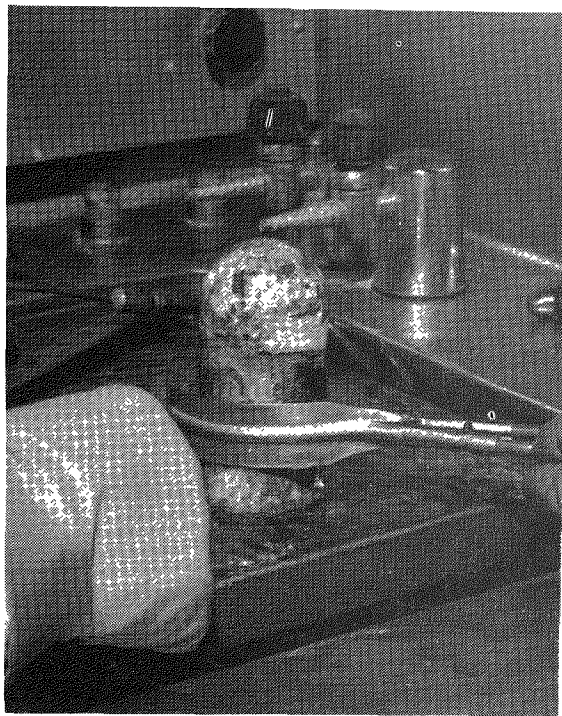
The capsule had a white deposit on the vent end (Photograph 11) and sides. A chemical analysis of this deposit is given in Table 1. Where the canister wall had disintegrated there were deposits of various colors, and this area was corroded (Photograph 12).

Salt deposits were removed from the surface of the vent end to obtain an O-ring seal while the capsule was stored in the chill block. The capsule was then placed in the water-cooled chill block, and the top

690098

L - 690110

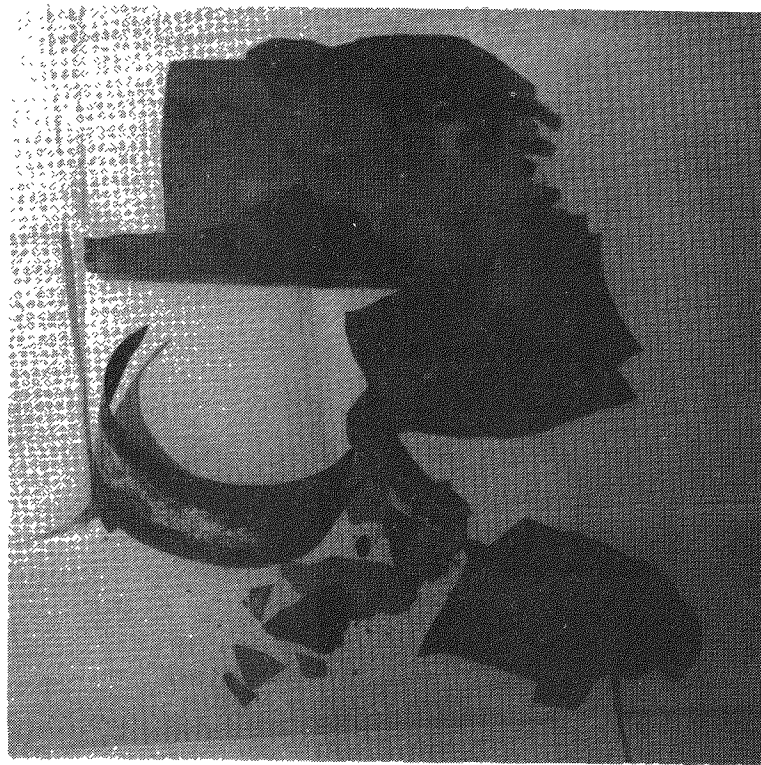
R - 690102



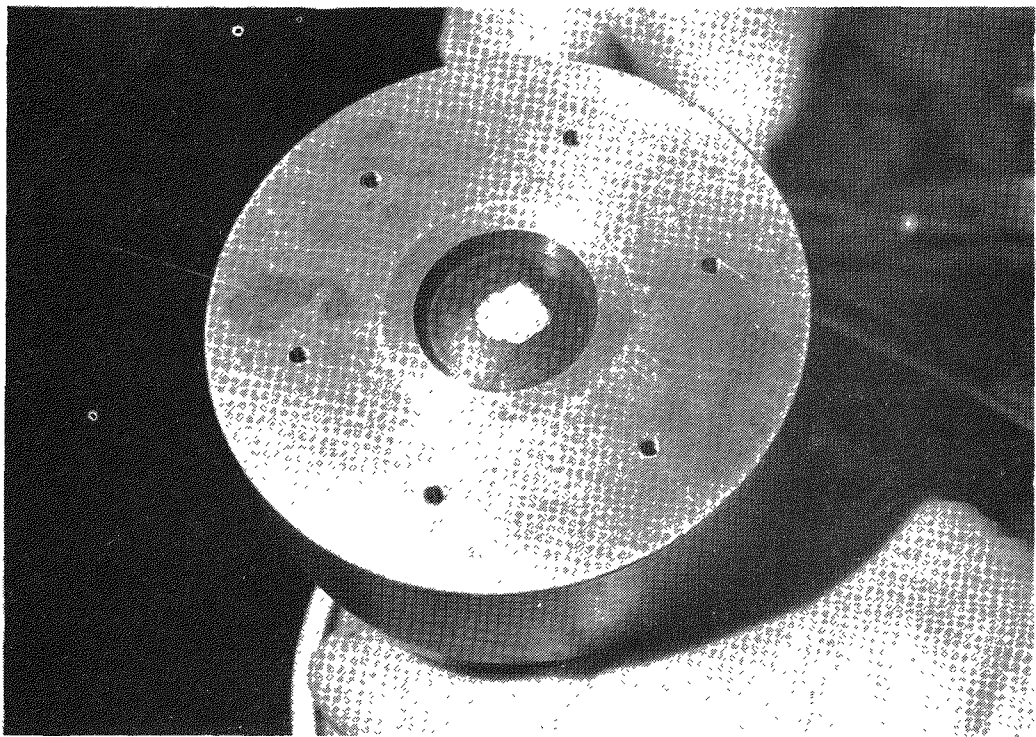
PHOTOGRAPH 8 - Canistered capsule completely removed from graphite heat shield.



PHOTOGRAPH 9 - Canistered capsule showing disintegrated portion of canister sleeve.



PHOTOGRAPH 10 - Canister pieces.



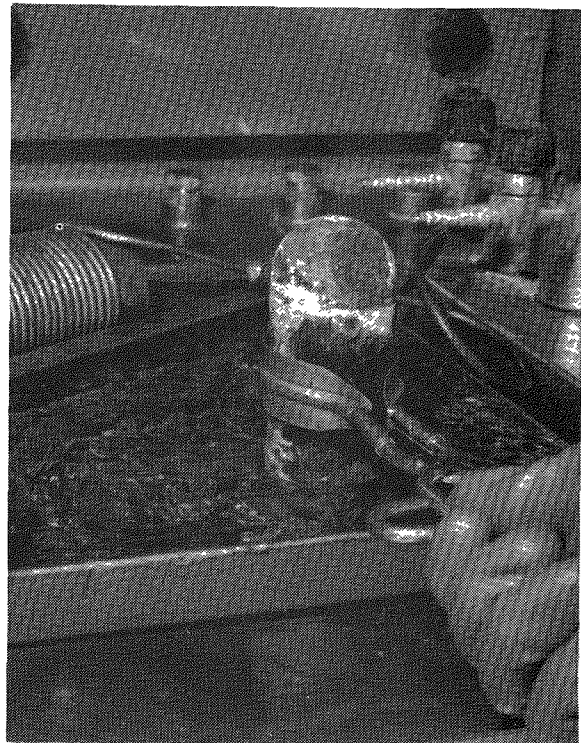
690103

PHOTOGRAPH 11 - Vent end of capsule.

Table 1

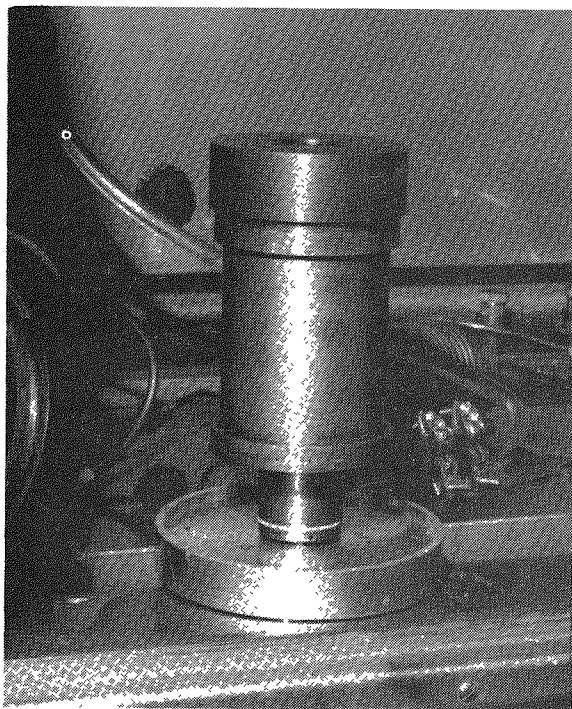
ANALYSIS OF WHITE DEPOSIT FROM  
VENT END OF CAPSULE 375/369

<u>Element</u>	<u>Wt %</u>	<u>Element</u>	<u>Wt %</u>
Fe	0.1	Al	0.1
B	0.004	Mo	>1.0
Si	0.9	Ca	Major
Mn	0.005	V	0.015
Pb	0.02	Cu	0.15
Ta	>1.0	Zr	>1.0
Mg	0.6	Na	0.2
Cr	0.15	Zn	0.05
W	0.15	Ti	0.09
Ni	0.2	Sr	0.9
Co	0.9	Ba	Trace



690111

PHOTOGRAPH 12 - Canistered capsule  
with various colored deposits on  
surface.



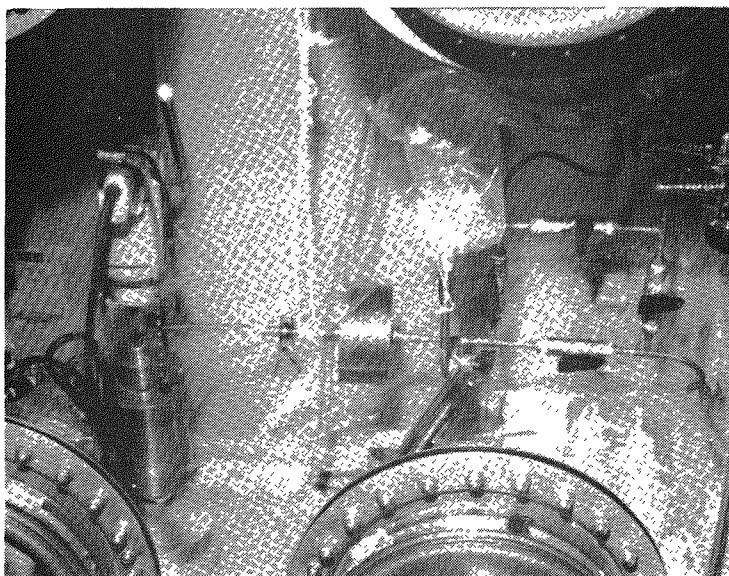
PHOTOGRAPH 13 - Container for storing the heat source after disassembly.

of the block was screwed into place (Photograph 13). A leak check fixture with an O-ring seal between the top of the chill block and the leak check adapter was fastened into position. A vacuum was pulled using an NRC mass spectrometer, and a measurement was made of the helium leak rate. It was difficult to determine the leak rate over that of the background but, after the system reached equilibrium, a rate was measured.

On January 14, 1969, the filter diaphragm was re-punctured in the same hole and with the same punch as was used in the assembly operation of December, 1967. The observed leak rate was roughly equivalent to the original leak rate. A white deposit could be seen in the punctured hole. A detailed metallographic and microprobe examination was performed on the filter. Results will be presented in a forthcoming communication.

#### D. Fuel Removal

On January 14, 1969, capsule SN 375/369 was placed into a special fixture designed and fabricated to utilize an 0.25 in. (0.635 cm) drill bit and also to serve as a funnel for pouring the free-flowing fuel from the capsule (Photograph 14). The entire assembly was transferred to an uncontaminated alpha box.



PHOTOGRAPH 14 - Fixturing inside box used for drilling the capsule, recording the internal pressure and collecting a gas sample.

An internal pressure measuring manifold was attached to the fixture (Figure 1), and the system was evacuated and leak-checked. When the system was leak-free, the drilling operation was initiated. After several minutes, a pressure rise was indicated on the Wallace-Tiernan gage. The gas in the system was allowed to equilibrate, and the pressure was noted. The gas was then expanded into a previously calibrated volume, and the pressure again was noted after equilibration. The calibrated volume was then removed from the system and submitted for gas analysis. Gas analysis results are given in Table 2.

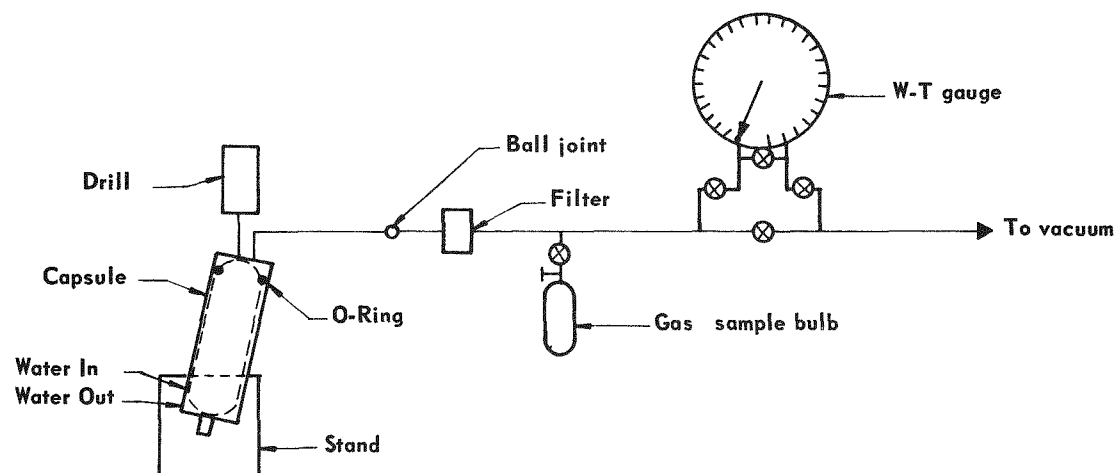


FIGURE 1 - Schematic drawing of internal pressure manifold.

Table 2  
ANALYSIS OF GAS RELEASED FROM  
CAPSULE SN 375/369

<u>Constituent</u>	<u>Vol %</u>
H <sub>2</sub>	0.0
<sup>3</sup> He	0.0
<sup>4</sup> He	73.1
H <sub>2</sub> O	0.0
N <sub>2</sub>	3.9
O <sub>2</sub>	1.0
Ar	21.9
CO <sub>2</sub>	0.0

The calculated internal pressures corresponding to two assumed "average capsule temperatures" are given in Table 3. The "average temperature" was derived from a theoretical temperature profile and was assumed to be (X + 165°C), where X is the surface temperature. Pressures were calculated for maximum (100°C) and minimum (25°C) surface temperatures.

After the pressure test was completed and the gas sample collected, the drill motor, drill press, internal pressure manifold, and Wallace-Tiernan gage were removed from the

alpha box and were found to be free from alpha contamination. This indicated that the manifold filter contained all the airborne <sup>238</sup>Pu particulate material. The manifold filter and housing were disconnected at the ball joint (Figure 1). The wipe count of the inside of the ball joint was about 12,000 counts/min. Subsequent evaluation of this filter by alpha pulse-height analysis showed 0.3 µg of <sup>238</sup>Pu. This indicated that very little airborne activity had been released when the capsule was punctured.

Table 3  
CALCULATED INTERNAL PRESSURE  
CORRESPONDING TO ASSUMED AVERAGE  
SURFACE TEMPERATURE  
OF CAPSULE 375/369

Assumed Average Surface Temp. (°C)	Internal Pressure (mm)
265	1000
190	850

in a plastic tent contained within a clean (free from alpha contamination) fumehood. These solutions were then processed for fines content in the same manner as the fines analysis of impact capsule #15.<sup>1</sup> Results of these fines analysis are given in Appendix B.

On January 16, 1969, the vent end of capsule SN 375/369 was cut off with a tubing cutter. The fuel was found to be sintered, as indicated previously by the radiographs, and took the shape of the inside of the capsule (Photograph 15). The glowing red, sintered clump appeared to be thicker in the mid-section than at the domed end (Photograph 16). There was no visible indication of salt inside the capsule. A sample of the sintered clump was taken for analytical

Free-flowing fuel in the capsule was poured out through the drill hole under water. Approximately 180 g of free-flowing fuel were removed. This fuel appeared to be similar in appearance to that originally loaded into the capsule. This fuel, on a 44  $\mu\text{m}$  screen, was washed with water (containing a wetting agent) until no visible material could be seen coming through the screen. The wash solutions, containing  $^{238}\text{Pu}$  particulate material less than 44  $\mu\text{m}$ , were removed from the glove box and placed



PHOTOGRAPH 15 - Upper portion of capsule exposing fuel.



PHOTOGRAPH 16 - Removal of agglomerated fuel.

examination and also for metallography. Analytical results are given in Appendix A; metallographic and microprobe findings are published in a separate report. The sintered fuel was broken up, put into fuel cans, and stored at Mound Laboratory.

E. General Comments

Capsule SN 375/369 was not calorimetered and neutron emission rates were not determined after removal of the capsule from the graphite heat assembly. This was the case since, in order to obtain such measurements, the capsule would have been allowed to heat up, and there would have been danger of capsule rupture due to a potentially plugged vent.

Slides containing fuel fines less than 10  $\mu\text{m}$  were sent to Tracerlab, and determination of the particle size distribution was made. Results are given in Appendix C.

An historical sample (#309) taken of the same fuel (SNAP-19B Dispersal Capsule SN 309), but before it was loaded into capsule SN 375/369, was washed for fines using the same technique as previously.<sup>1</sup> The results are presented in Appendix B. Slides of material less than 10  $\mu\text{m}$  were prepared and sent to Tracerlab. Results of the determination are shown in Appendix D.

The filter was machined out of capsule SN 375/369 and flow-tested in a special test fixture. Upon completion of this test, the filter was subjected to a metallographic examination and microprobe analysis. Results are still pending.

#### IV. DISASSEMBLY OF HEAT SOURCE SN 361/368

A. Graphite Heat Shield

The graphite heat shield was removed from the second SNAP-19B (IRHS) unit on January 20, 1969. The operation was begun by removing the graphite heat accumulator block from around the graphite heat shield (Photographs 17-19). Salt deposits were present on the outside of the heat shield (Photograph 20). The graphite heat shield was visually inspected and no cracks could be seen. Dimensions were determined using a vernier caliper; but due to the various surface deposits as stated previously (Section III-A) it was difficult to obtain a comparison with the original dimensions. No alpha contamination was detected. The source was then placed into a holder. Several attempts were made to unscrew the heat shield, but each ended in failure (Photographs 21 and 22). The heat source was then put into a fume-hood, and the graphite heat shield was carefully broken from around

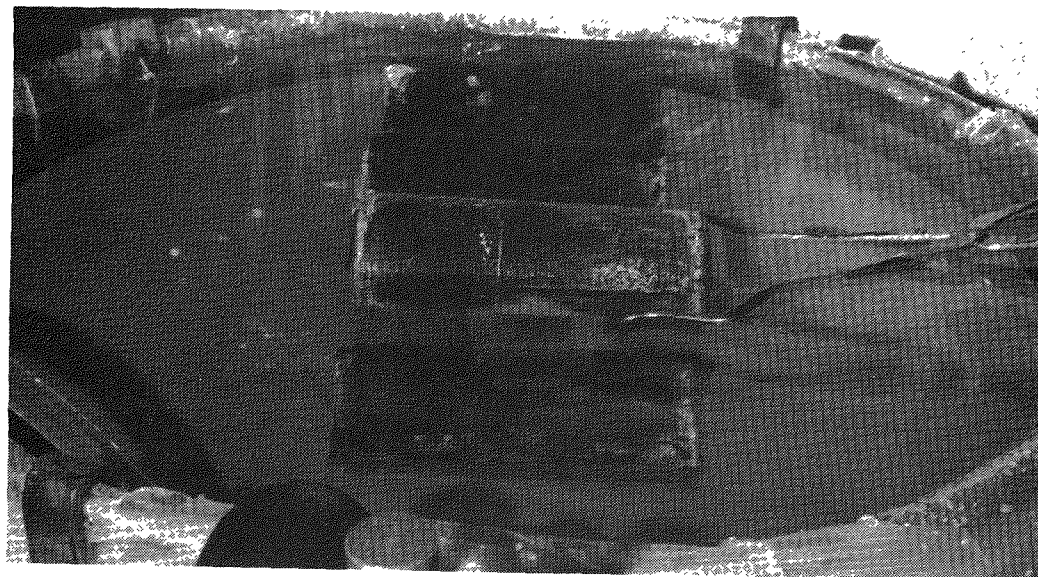
the canistered capsule using a hammer and screwdriver. Photographs 23-28 illustrate the sequence of this breaking-off operation. The coating on the inside of the graphite heat shield was not attached to the mid-section of the graphite. Water was found on the inside of the heat shield.

690425

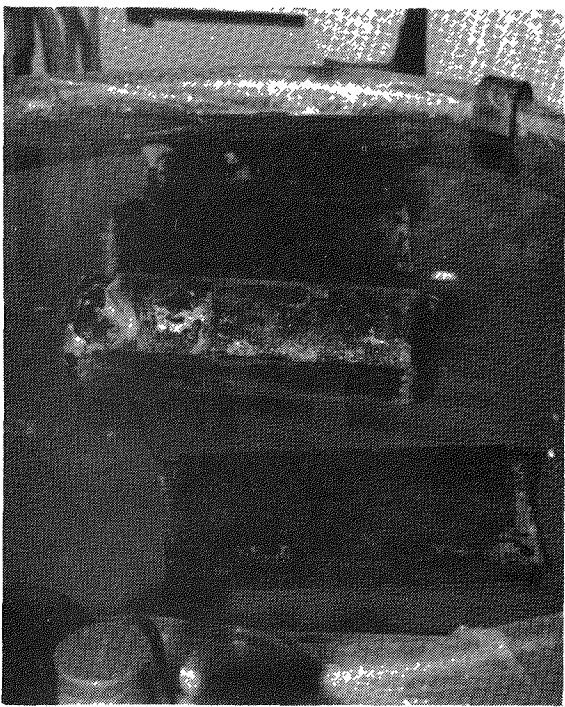


PHOTOGRAPH 17 - Removal of heat accumulator block from heat source SN 361/368.

690432



PHOTOGRAPH 18 - Heat source SN 361/368 with heat accumulator block off.



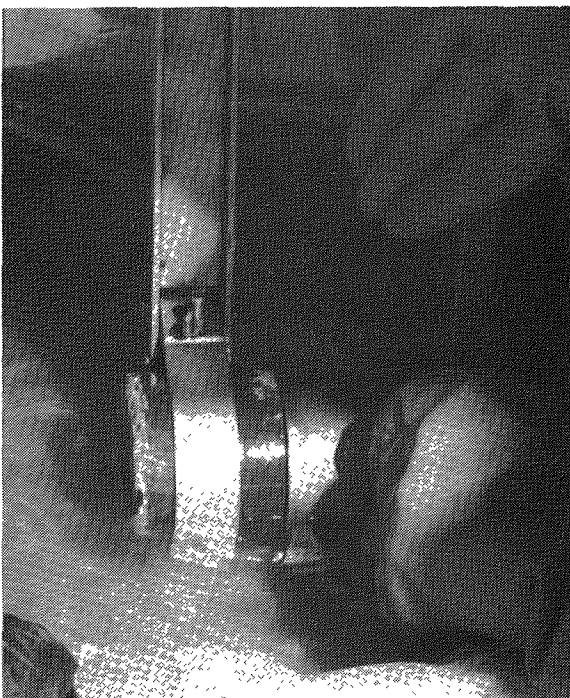
PHOTOGRAPH 19 - Heat source SN 361/368 with heat accumulator block off (90° from Photograph 18).



PHOTOGRAPH 20 - Heat source SN 361/368 with heat accumulator block off (180° from Photograph 18).



PHOTOGRAPH 21 - Use of strap wrenches to unscrew the graphite block.



PHOTOGRAPH 22 - Use of strap wrenches to unscrew the graphite block.

L - 690415 R - 690429

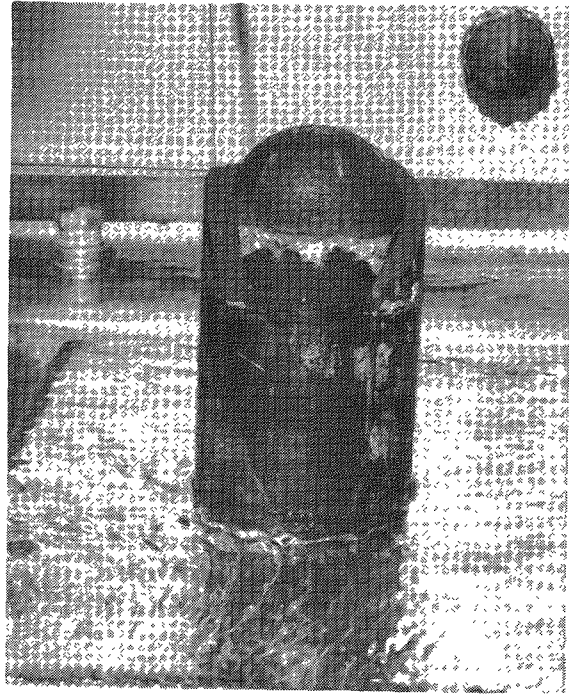
L - 690412 R - 690428

L - 690424      R - 690422

L - 690427      R - 690401



PHOTOGRAPH 25 - Exposed canistered capsule.



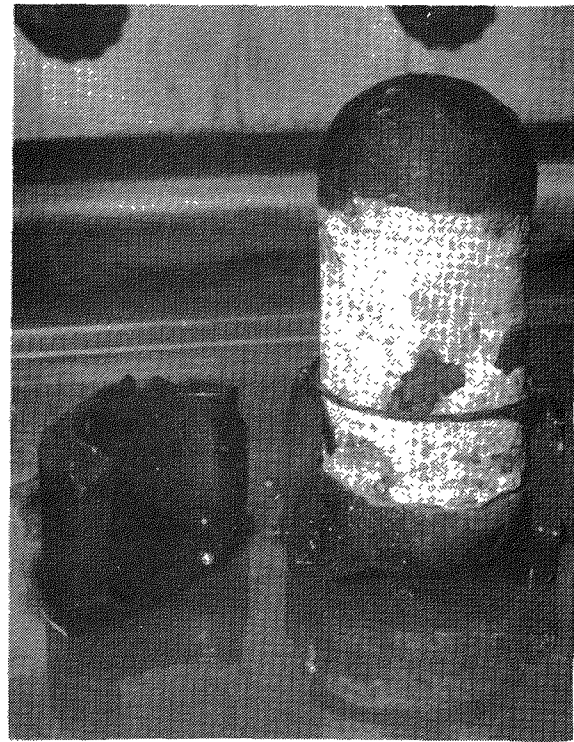
PHOTOGRAPH 23 - Exposed canistered capsule with tantalum pad stuck to domed end.



PHOTOGRAPH 26 - Exposed canistered capsule.



PHOTOGRAPH 27 - Exposed canistered capsule.



PHOTOGRAPH 28 - Exposed canistered capsule.

B. Canister

Upon removal of the canistered capsule from the broken heat shield, parts of the compliance pads were found to be stuck to each domed end of the canister (Photograph 23). Salt deposits were on the canister. The cap and sleeve portions were removed intact except for a small area around the top of the sleeve portion (Photograph 29) which had to be broken to initiate canister sleeve removal (Photograph 30). The coating on the inside surface appeared to be intact and the canister was embrittled. Photographs 31 and 32 show the various components removed from around the capsule. All the components that were removed were found to be free from contamination.

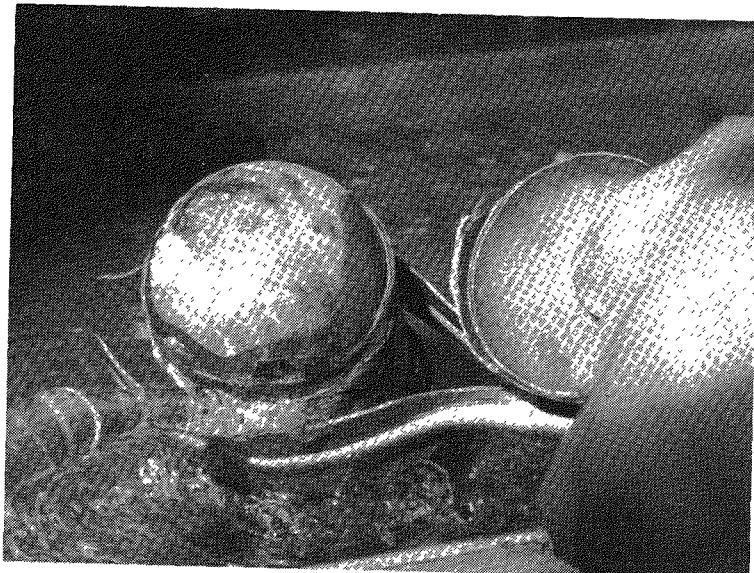


PHOTOGRAPH 29 - Exposed canistered capsule showing area that was broken to initiate canister sleeve removal.

L - 690421      R - 690423

690405

690420

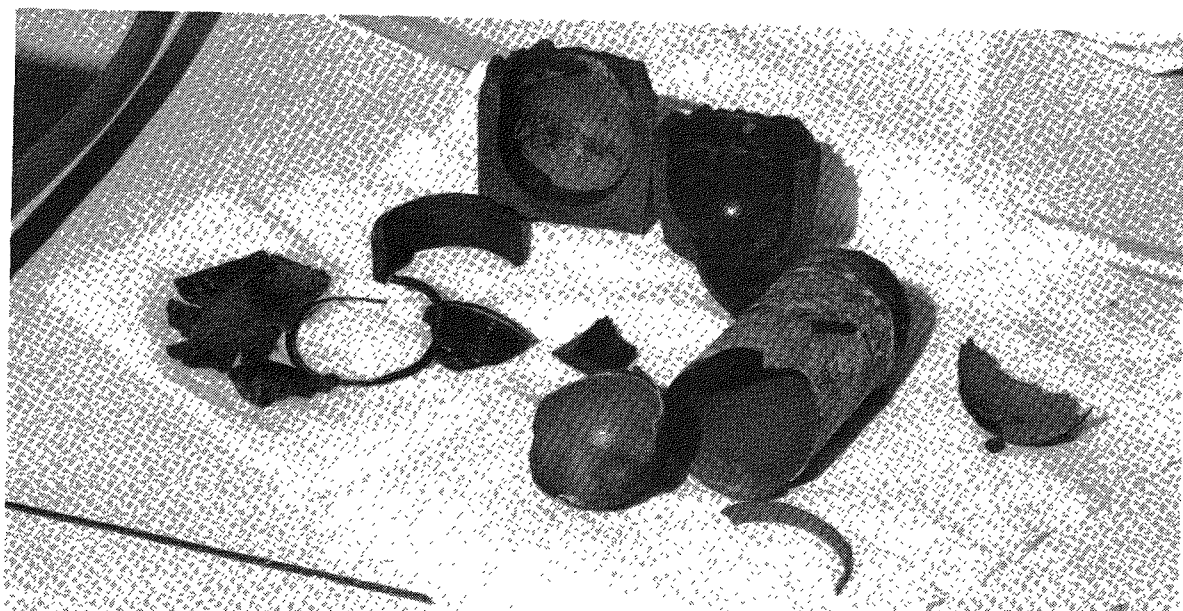


PHOTOGRAPH 30 - Exposed domed vent end with canister cap removed.

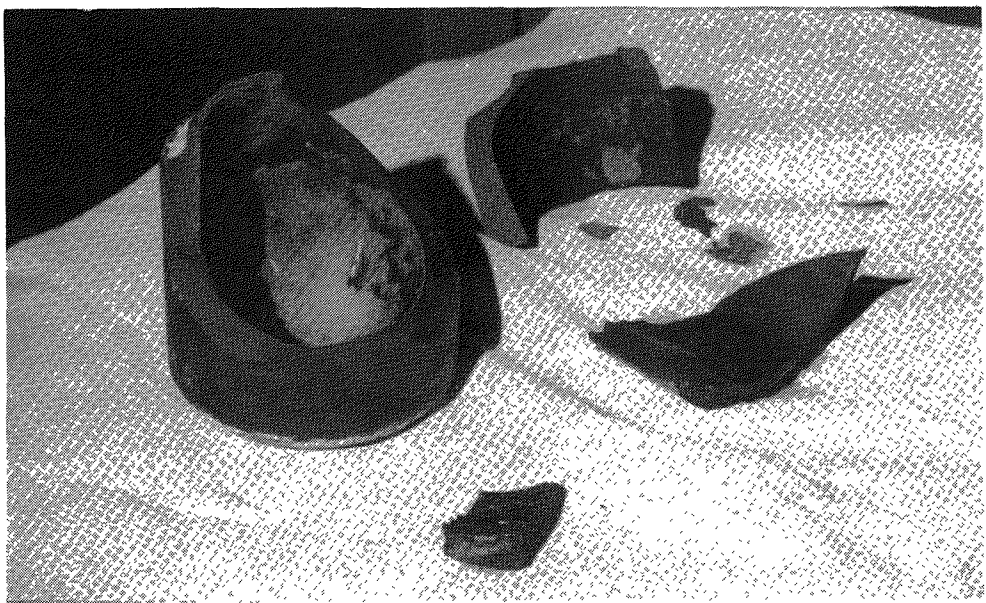
C. Capsule

There was no noticeable surface corrosion on the capsule as was the case with capsule 375/369. There were some greenish streaks running the length of the capsule and white deposits on various areas of the capsule surface (Photographs 33 and 34). The filter diaphragm area was not caked with white deposits (Photograph 30) as previously noted on capsule SN 375/369.

690399

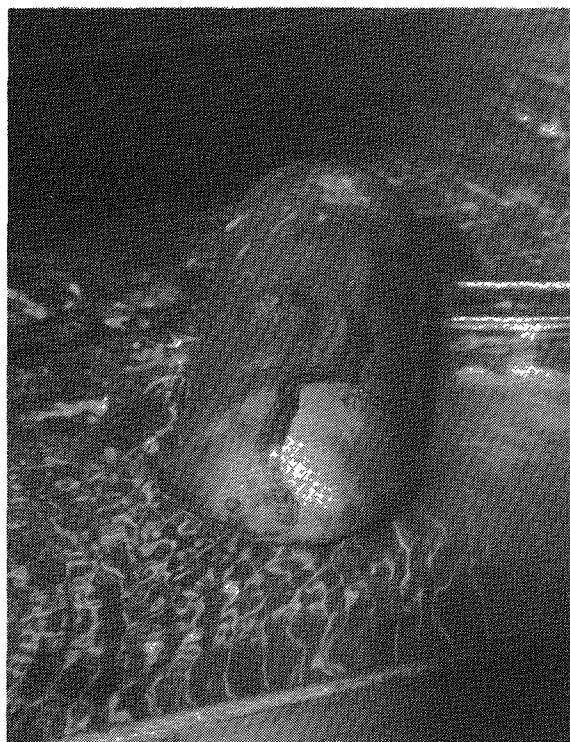


PHOTOGRAPH 31 - Capsule components after removal.

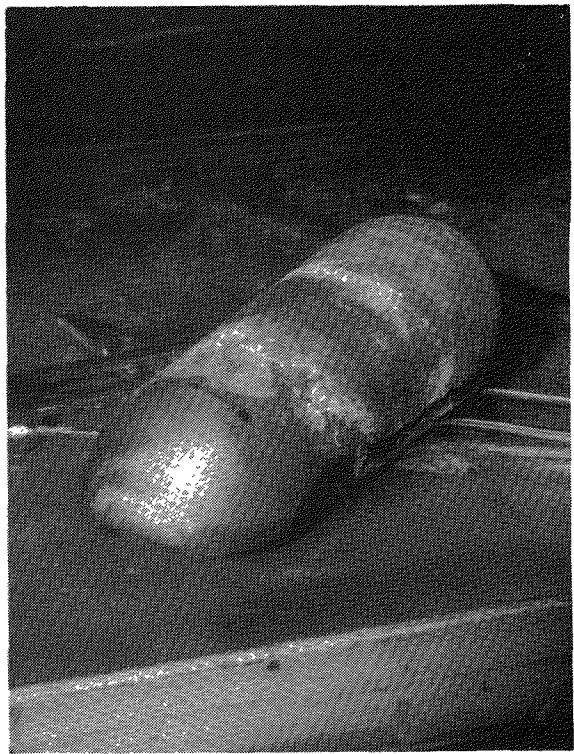


PHOTOGRAPH 32 - Graphite heat shield section.

690426



PHOTOGRAPH 33 - Capsule showing green streaks.



PHOTOGRAPH 34 - Capsule with canister removed.

L - 690419 R - 690402

#### D. Fuel Removal

The capsule was transferred to a chill block, and the fixture was fastened to the top of the block. The assembly was then placed into a glove box free from alpha contamination. The same type of drilling fixture as used in opening capsule SN 375/369 was used for drilling capsule SN 361/368. After the drilling operation, the chill block with capsule was fastened to a pouring stand.

Figure 2 shows a schematic illustration of the operation which followed. The capsule was inverted, and ~10 g of fuel came out into the elutriation column (Photograph 35). This operation was repeated

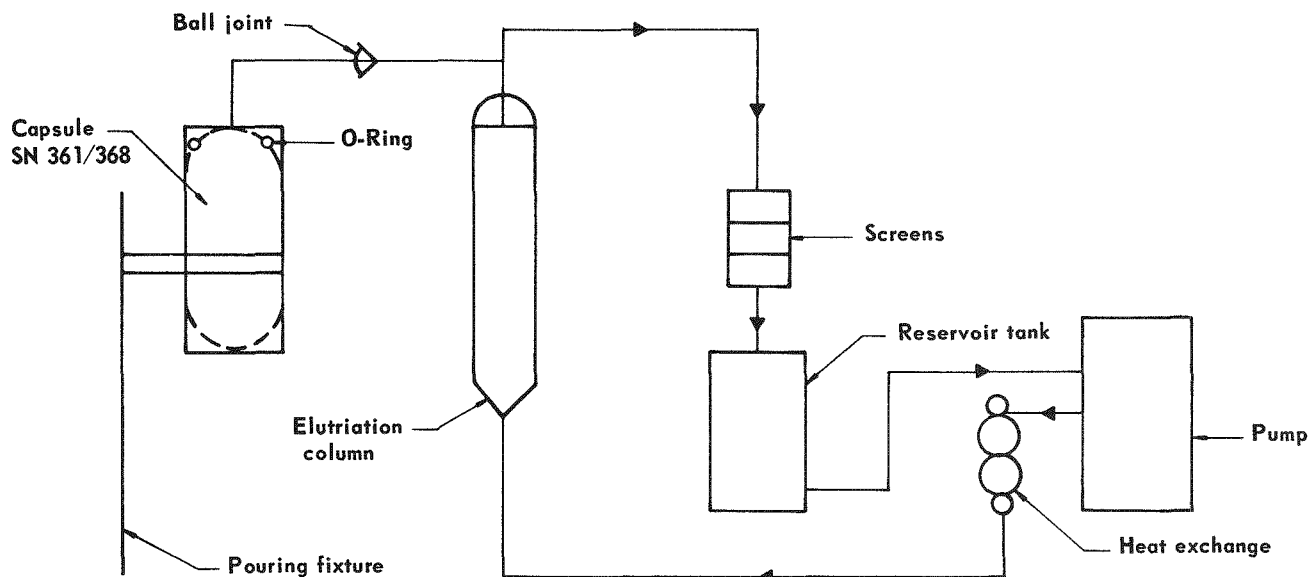


FIGURE 2 - Schematic drawing of elutriation wash apparatus for fines determination.

several times until no more free-flowing fuel came out of the capsule through the drill hole. This free-flowing fuel was then washed with approximately five liters of water, and all the  $^{238}\text{Pu}$  particulate material less than 44  $\mu\text{m}$  was caught on the 20  $\mu\text{m}$  and 10  $\mu\text{m}$  screens. This material was then washed off each screen, and each screen was cut out and dissolved. The solutions were boiled down to  $\sim 1000$  ml and then submitted for an alpha pulse-height analysis to determine how much  $^{238}\text{Pu}$  was present in the 44-20  $\mu\text{m}$ , 20-10  $\mu\text{m}$ , and less than 10  $\mu\text{m}$  size ranges. Results of this fines analysis are presented in Appendix B. Material less than 10  $\mu\text{m}$  in diameter was mounted on slides and sent to Tracerlab for determination of particle size distribution. Results are given in Appendix E.

On January 24, 1969, the vent end of capsule SN 361/368 was cut off with a tube cutter. The fuel was sintered, but the large clump had broken into several pieces (Photographs 36 and 37). This probably occurred during removal of the graphite heat shield from around the capsule because preliminary radio-graphs had shown the fuel bed to be intact.

All of the fuel was removed from the capsule and placed into fuel cans for storage at Mound Laboratory. A sample of the sintered fuel was taken for metallographic and microprobe analyses. Results were similar to those observed for the sintered fuel from capsule SN 375/369. A sample of fuel was also analyzed and results are given in Appendix A.

#### E. General Comments

Capsule 361/368 was not calorimetered and neutron emission rates were not determined after removal of the capsule from the canister, for the same reason given in Section III-E of this report.

The filter was machined out of the capsule and flow-checked in a special test fixture. Upon completion of the flow test, the filter was subjected to metallographic and microprobe analyses. Results are still pending and will be presented in a forthcoming communication.



PHOTOGRAPH 35 - Elutriation column containing  $^{238}\text{PuO}_2$  microspheres.

690413

R - 690411  
L - 690407



PHOTOGRAPH 36 - Capsule vent end lifted up to show exposed fuel.



PHOTOGRAPH 37 - Capsule vent end removed to show exposed fuel.

#### V. ACKNOWLEDGMENT

The disassembly and inspection operations at Mound Laboratory relative to the two recovered SNAP-19B (IRHS) heat sources required extensive team effort and use of many disciplines. The authors of the present report wish to acknowledge all contributions made to this program by their associates in the Nuclear Operations Division, and particularly by those in the Production and Technology Departments. Appreciation is likewise extended to various engineering groups at Mound Laboratory - also to the Atomic Energy Commission, Dayton Area Office - for their assistance.

#### VI. REFERENCES

1. P. H. Bonnell, Fines Analysis of Plutonium Dioxide Microspheres After Impact, MLM-1626 (April 18, 1969), 21 pp.

This page  
intentionally  
left blank

## APPENDIX A

### RESULTS OF CHARACTERIZATION OF FREE-FLOWING FUEL FROM CAPSULES 375/369 AND 361/368

Table 1  
CHARACTERIZATION OF FREE-FLOWING FUEL FROM CAPSULE SN 375/369

<u>Property</u>	<u>Amount</u>	<u>Property</u>	<u>Amount</u>
Apparent Density (g/cc)	9.68	Melting Point of Free Flowing Material (°C)	2420 ± 80
Crush Strength (g)	80 Mesh - 310 100 Mesh - 266 140 Mesh - 168	Melting Point of Lump (°C)	2435 ± 80
Shape ( $\frac{L}{D} < 2$ )	Acceptable	Cation Impurities (wt %, as metal)	
Size (%) (50 $\mu\text{m}$ -250 $\mu\text{m}$ )	99.997	Si	0.34
Stoichiometry (O:Pu)	2.00 (No other phases detected)	Ni	0.05
<u>Plutonium (wt % Pu)</u>		Fe	0.26
238	79.08	Sn	Trace
239	16.48	Al	0.06
240	3.40	Zr	0.01
241	0.86	Ca	0.06
242	0.17	B	0.02
236	0.81 ppm	Mn	0.01
<u>Actinides (wt % of PuO<sub>2</sub>)</u>		Cr	0.03
Mass #		Cu	0.02
227	<0.010	Ti	0.01
231	<0.010	Co	0.03
232	0.200	Mg	0.04
233	<0.010	Zn	0.02
234	1.180	Na <sup>a</sup>	2.00 ppm
235	<0.010	Total	0.96%
236	<0.002		
237	0.125		
Am 241	814 ppm		

<sup>a</sup> Analysis made on sample of fuel that had not been washed.

Table 2  
CHARACTERIZATION OF FREE-FLOWING FUEL FROM CAPSULE SN 361/368

Property	Amount	Property	Amount
Apparent Density (g/cc)	10.20	Melting Point of Free Flowing Material (°C)	2360 ± 80
Crush Strength (g)	80 Mesh - 282 100 Mesh - 313 140 Mesh - 266	Melting Point of Lump (°C)	2375 ± 80
Shape ( $\frac{L}{D} < 2$ )	Acceptable	Cation Impurities (wt %, as metal)	
Size (%) (50 µm-250 µm)	100	Si	0.06
Stoichiometry (O:Pu)	2.00 (no other phases detected)	Ni	0.24
Plutonium (wt % Pu)		Fe	0.09
238	80.12	Al	0.12
239	15.85	Ca	0.14
240	3.036	B	0.02
241	0.857	Mn	0.0
242	0.133	Cr	0.02
236	0.7 ppm	Cu	0.11
Actinides (wt % of PuO <sub>2</sub> )		Co	<0.02
Mass #		Mg	0.06
227	<0.010	Zn	<0.02
231	<0.010	Na <sup>a</sup>	<u>0.8 ppm</u>
232	<0.010	Total	0.90
233	<0.001		
234	1.229		
235	<0.001		
236	<0.0005		
237	0.081		
Am 241	691 ppm		

<sup>a</sup> Analysis made on sample of fuel  
that had not been washed.

This page  
intentionally  
left blank

APPENDIX B

SUMMARY OF FINES DATA FOR  
CAPSULES SN 375/369, 361/368, AND 309

Table 1

## FINES DATA FOR CAPSULE SN 375/369

	<u>0-10 <math>\mu\text{m}</math></u>	<u>10-20 <math>\mu\text{m}</math></u>	<u>20-44 <math>\mu\text{m}</math></u>	<u>Total 0-44 <math>\mu\text{m}</math></u>
Radiochemical Analysis (g $^{238}\text{Pu}$ )	0.016	0.039	0.319	0.374
Fume Hood Filter (g $^{238}\text{Pu}$ ) <sup>a</sup>	0.000021	--	--	0.000021
Support Hardware (g $^{238}\text{Pu}$ )	0.005	0.013	0.030	0.048
Glovebox Filter (g $^{238}\text{Pu}$ ) <sup>a</sup>	0.000010	--	--	0.000010
Manifold Filter (g $^{238}\text{Pu}$ ) <sup>a</sup>	<u>0.0000003</u>	--	--	<u>0.0000003</u>
Total (g $^{238}\text{Pu}$ )	0.0210313	0.052	0.349	0.422
Total Wt % Fines Based on Free-Flowing Fuel <sup>b</sup>	0.016	0.040	0.268	0.324
Total Wt % Fines Based on Capsule Inventory <sup>c</sup>	0.0021	0.0052	0.035	0.0423

<sup>a</sup> Material on filter assumed to be less than 10  $\mu\text{m}$ .<sup>b</sup> Based on 130.16 g  $^{238}\text{Pu}$ .<sup>c</sup> Based on 1010.0 g  $^{238}\text{Pu}$ .

Table 2

## FINES DATA FOR CAPSULE SN 361/368

	<u>0-10 <math>\mu\text{m}</math></u>	<u>10-20 <math>\mu\text{m}</math></u>	<u>20-44 <math>\mu\text{m}</math></u>	<u>Total 0-44 <math>\mu\text{m}</math></u>
Radiochemical Analysis (g $^{238}\text{Pu}$ )	0.0016	0.024	0.276	0.302
Fines from Support Hardware (g $^{238}\text{Pu}$ )	<u>0.0003</u>	<u>0.0050</u>	<u>0.0576</u>	<u>0.063</u>
Total (g $^{238}\text{Pu}$ )	0.0019	0.029	0.3336	0.365
Total Wt % Fines Based on Free-Flowing Fuel <sup>a</sup>	0.004	0.063	0.729	0.796
Total Wt % Fines Based on Capsule Inventory <sup>b</sup>	0.0002	0.0029	0.033	0.036

<sup>a</sup> Based on 45.8 g  $^{238}\text{Pu}$ .<sup>b</sup> Based on 998.2 g  $^{238}\text{Pu}$ .

Table 3  
FINES DATA FOR SN 309

	<u>0-10 <math>\mu\text{m}</math></u>	<u>10-20 <math>\mu\text{m}</math></u>	<u>20-44 <math>\mu\text{m}</math></u>	<u>Total 0-44 <math>\mu\text{m}</math></u>
Radiochemical Analysis (g $^{238}\text{Pu}$ )	0.000073	0.000081	0.00532	0.005474
Fume Hood Filter (g $^{238}\text{Pu}$ )	0.000022	--	--	0.000022
Support Hardware (g $^{238}\text{Pu}$ )	<u>0.000018</u>	<u>0.000015</u>	<u>0.000999</u>	<u>0.001032</u>
Total (g $^{238}\text{Pu}$ )	0.000113	0.000096	0.006319	0.00653
Total Wt % Fines <sup>a</sup>	0.0036	0.0031	0.200	0.210

<sup>a</sup> Based on sample weight of 3.142 g  $^{238}\text{Pu}$ .

This page  
intentionally  
left blank

## APPENDIX C

### SUMMARY REPORT OF PLUTONIUM-238 PARTICULATE MATERIAL LESS THAN 10 $\mu\text{m}$ IN SIZE AS REMOVED FROM FREE-FLOWING FUEL CONTAINED IN CAPSULE 375/369

Walter Holland, Tracerlab

A Division of Laboratory for Electronics, Inc.  
2030 Wright Ave., Richmond, California

We have completed analysis of the particulate fragments in the less than 10  $\mu$  sieved fraction of sample 19-1. The analysis procedure used was the same as described in earlier reports.<sup>(1-3)</sup> The results of radiochemical analyses of the sized batches of radioactive particles having equivalent circular diameters larger than 2  $\mu$  are presented as Table I. Also included in Table I are the equivalent  $^{238}\text{PuO}_2$  spherical diameters for the size ranges and mid-ranges of these measurements. The results of the hollow-star exposures for particles having equivalent  $^{238}\text{PuO}_2$  spherical diameters between about 2 and 0.1  $\mu$  are included as Table II. The equivalent  $^{238}\text{PuO}_2$  mass of particles having spherical diameters less than 0.1  $\mu$  is calculated as follows:

$^{238}\text{PuO}_2$ in particles on the slides from which >2 $\mu$ particles have been isolated (see Table I)	$51.5 \times 10^{-3}$ $\mu\text{g}$
$^{238}\text{PuO}_2$ in particles with equivalent $^{238}\text{PuO}_2$ spherical diameters from 0.1 to 2.06 $\mu$ (see Table II)	$-26.5 \times 10^{-3}$ $\mu\text{g}$
$^{238}\text{PuO}_2$ in particles with equivalent $^{238}\text{PuO}_2$ spherical diameters <0.1 $\mu$ .	$25.0 \times 10^{-3}$ $\mu\text{g}$

In Table III the values are presented which show the numerical size distribution of radioactive particles in the <10  $\mu$  sieved fraction of sample 19-1. Table IV contains the mass percentages per size range for radioactive particles in the less than 10  $\mu$  sieved fraction of sample 19-1.

The mass percent and cumulative mass percent values listed in Table IV are used to calculate the percentages of the total impacted mass (including the cumulative percentages) which are listed in Table V. These values are combined with the Table VI values which were obtained from Dr. S. Abrahamson of Mound Laboratory and then plotted as Figure 1. From Figure 1 it is evident that 99.68% of the mass of microspheres which were impacted remains in particles with equivalent spherical diameters greater than 44  $\mu$ . Also  $3 \times 10^{-3}\%$  of the mass is found in particles with spherical diameters less than 0.1  $\mu$ .

1. Particle Analysis of Radioactive Fragments with Diameters <20  $\mu$  from Impacted Sample 3, W. Holland, Tracerlab, a division of Laboratory for Electronics, for Sandia Corporation, September 16, 1968.
2. Particle Analysis of Radioactive Fragments with Diameters <20  $\mu$  from Impacted Sample 5, W. Holland, Tracerlab, a division of Laboratory for Electronics, for Sandia Corporation, September 17, 1968.
3. Particle Analysis of Radioactive Fragments with Diameters <10  $\mu$  from Impacted Sample 15, W. Holland, Tracerlab, a division of Laboratory for Electronics, for Sandia Corporation, October 23, 1968.

TABLE I RESULTS OF RADIOCHEMICAL ANALYSIS - SAMPLE 19-1

Size Range ( $\mu$ )	Equivalent $^{238}\text{PuO}_2$ Spherical Diameters	Midrange ( $\mu$ )	Equiv. Circular Diameter Size Range ( $\mu$ )	Number of Particles per SSize Range	Equiv. $^{238}\text{PuO}_2$ Mass per Size Range ( $\mu\text{g}$ )
-	-	-	<2.0	-	$51.5 \times 10^{-3}$
1.02-2.06	1.54		2.0-4.0	725	$16.10 \times 10^{-3}$
2.06-3.19	2.33) 2.59 2.85)		4.0-6.0 6.0-8.0	156) 176 20)	$11.80 \times 10^{-3}$ $2.79 \times 10^{-3}$
3.19-4.39	3.59) 3.79 3.99)		8.0-10.0 10.0-12.0	3) 4 1)	$0.833 \times 10^{-3}$ $0.380 \times 10^{-3}$
			Totals	905	$83.4 \times 10^{-3}$

TABLE II NORMALIZED RESULTS OF MEASURING SAMPLE 19-1 PARTICLES  
BY THE HOLLOW STAR TECHNIQUE

Size Range ( $\mu$ )	Equivalent $^{238}\text{PuO}_2$ Spherical Diameters	Midrange ( $\mu$ )	Number per Size Range	Equivalent $^{238}\text{PuO}_2$ Mass per Size Range ( $10^{-10}$ gms)
0.1 -0.14	0.12		29,440	3.0559
0.14-0.21	0.18		42,880	15.0080
0.21-0.30	0.26		26,880	28.3853
0.30-0.42	0.36		9,760	27.2890
0.42-0.61	0.52		6,400	53.9904
0.61-0.88	0.74		2,800	68.0736
0.88-1.02	0.95		320	16.4621
1.02-2.06	1.54		240	52.5888
		Totals	118,720	264.8531

TABLE III NUMERICAL PERCENTAGES PER SIZE RANGE FOR RADIOACTIVE  
PARTICLES IN THE LESS THAN  $10 \mu$  SIEVED FRACTION OF SAMPLE 19-1

Equivalent $^{238}\text{PuO}_2$ Spherical Diameters	Size Ranges ( $\mu$ )	Equiv. Circular Diameter Size Ranges	No. of Particles per Size Range	Frequency Percent per Size Range	Cumulative Numerical Percent per Size Range
Size Ranges ( $\mu$ )	Midranges ( $\mu$ )	Size Ranges	Size Range	Size Range	Size Range
0.1 -0.14	0.12		29,440	24.61	24.61
0.14-0.21	0.18		42,880	35.84	60.45
0.21-0.30	0.26		26,880	22.47	82.92
0.30-0.42	0.36		9,760	8.16	91.08
0.42-0.61	0.52		6,400	5.35	96.43
0.61-0.88	0.74		2,800	2.34	98.77
0.88-1.02	0.95		320	0.27	99.04
1.02-2.06	1.54	2.0- 4.0	965	0.80	99.84
2.06-3.19	2.33) 2.59 2.85)	4.0- 6.0 6.0- 8.0	156) 176 20)	0.15	99.99
3.19-4.39	3.59) 3.79 3.99)	8.0-10.0 10.0-12.0	3) 4 1)	0.01	100.00
		Total	119,625		

TABLE IV MASS PERCENTAGES PER SIZE RANGE FOR RADIOACTIVE PARTICLES  
IN THE LESS THAN  $10 \mu$  SIEVED FRACTION OF SAMPLE 19-1

Size Ranges ( $\mu$ )	Equivalent $^{238}\text{PuO}_2$ Spherical Diameters	Midranges ( $\mu$ )	Equiv. Circular Diameter Size Ranges ( $\mu$ )	Mass per Size Range ( $10^{-10}$ g)	Mass Percent per Size Range	Cumulative Mass Percent per Size Range
<0.1		0.05		250.	29.98	29.98
0.1 - 0.14		0.12		3.06	0.37	30.35
0.14-0.21		0.18		15.01	1.80	32.15
0.21-0.30		0.26		28.38	3.40	35.55
0.30-0.42		0.36		27.29	3.27	38.82
0.42-0.61		0.52		53.99	6.47	45.29
0.61-0.88		0.74		68.07	8.16	53.45
0.88-1.02		0.95		16.46	1.98	55.43
1.02-2.06		1.54	2.0- 4.0	213.59	25.61	81.04
2.06-3.19	2.33) 2.85)	2.59	4.0- 6.0 6.0- 8.0	118.0) 27.9) 145.90	17.50	98.54
3.19-4.39	3.59) 3.99)	3.79	8.0-10.0 10.0-12.0	8.33) 3.80) 12.13	1.46	100.00
			Total	833.8831		

TABLE V MASS PERCENTAGES OF MICROSPHERES IN THE  $<10 \mu$  SIEVED SIZE RANGE

Equivalent $^{238}\text{PuO}_2$ Spherical Diameter Size Ranges ( $\mu$ )	Equivalent Circular Diameter Size Ranges ( $\mu$ )	Mass Percent per Size Range	Cumulative Mass Percent per Size Range	Basis - 0.01% of Micro- spheres Impacted are in $<10 \mu$ Sieved Fraction	
				Mass Percent per Size Range	Cumulative Percent Mass
<0.1		29.98	29.98	$2.998 \times 10^{-3}$	$2.998 \times 10^{-3}$
0.1- 0.14		0.37	30.35	$3.700 \times 10^{-5}$	$3.035 \times 10^{-3}$
0.14-0.21		1.80	32.15	$1.800 \times 10^{-4}$	$3.215 \times 10^{-3}$
0.21-0.30		3.40	35.55	$3.400 \times 10^{-4}$	$3.555 \times 10^{-3}$
0.30-0.42		3.27	38.82	$3.27 \times 10^{-4}$	$3.882 \times 10^{-3}$
0.42-0.61		6.47	45.29	$6.47 \times 10^{-4}$	$4.529 \times 10^{-3}$
0.61-0.88		8.16	53.45	$8.16 \times 10^{-4}$	$5.345 \times 10^{-3}$
0.88-1.02		1.98	55.43	$1.98 \times 10^{-4}$	$5.543 \times 10^{-3}$
1.02-2.06	2-4	25.61	81.04	$2.561 \times 10^{-3}$	$8.104 \times 10^{-3}$
2.06-3.19	4-8	17.50	98.54	$1.750 \times 10^{-3}$	$9.854 \times 10^{-3}$
3.19-4.39	8-12	1.46	100.00	$1.46 \times 10^{-4}$	$1.000 \times 10^{-2}$

TABLE VI RESULTS OF SIEVING MICROSPHERES IN SAMPLE 19-1

Sieved Size Range ( $\mu$ )	Mass Percent	Cumulative Percent
<10	0.01	0.01
10-20	0.04	0.05
20-44	0.27	0.32
<44	99.68	100.00

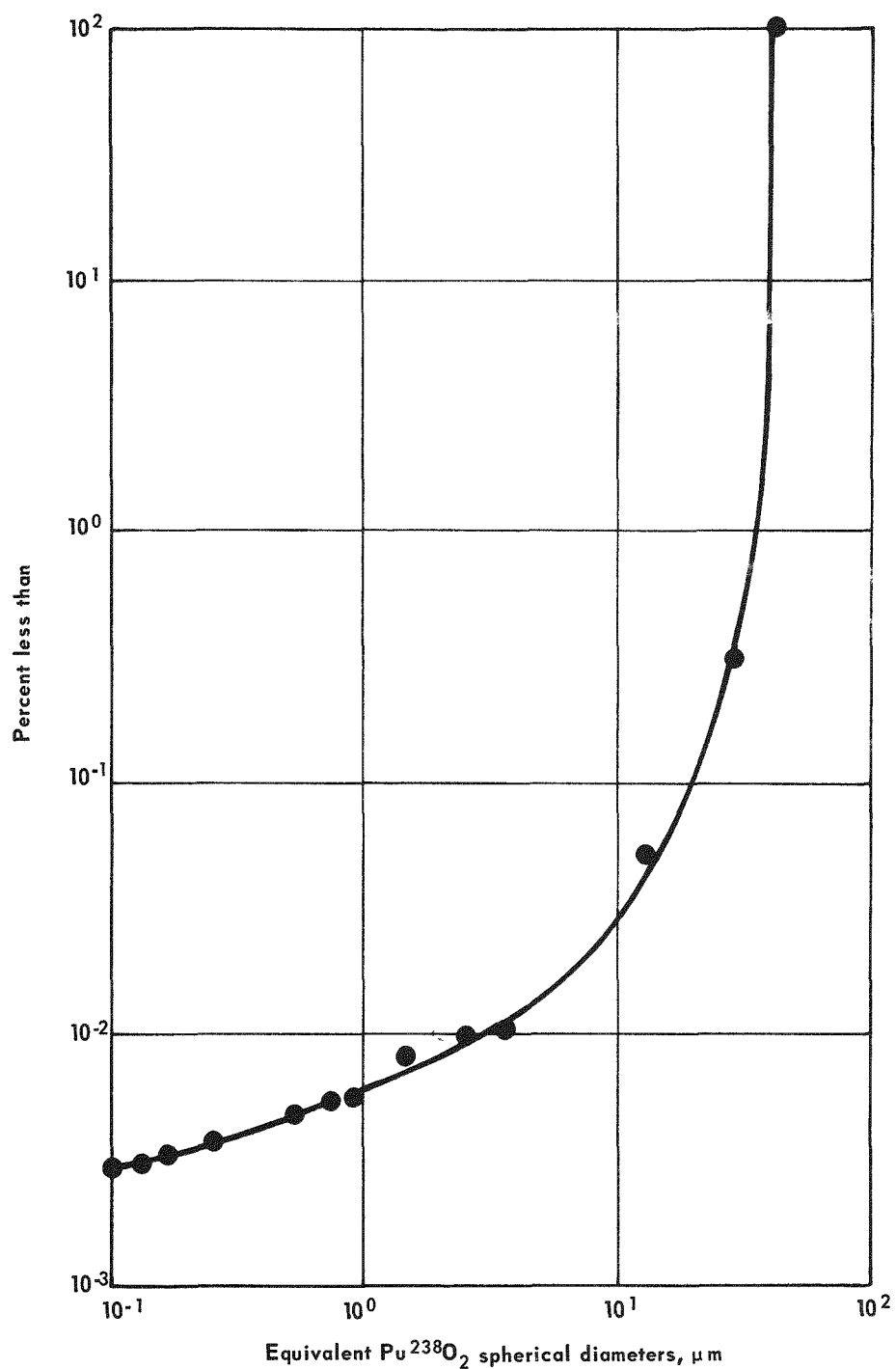


FIGURE 1 - Cumulative plot of mass percentages of all microspheres impacted in sample 19-1.

This page  
intentionally  
left blank

APPENDIX D

SUMMARY REPORT OF PLUTONIUM-238 PARTICULATE  
MATERIAL LESS THAN 10  $\mu$  IN SIZE AS REMOVED FROM  
HISTORICAL SAMPLE # 309

Walter Holland, Tracerlab

A Division of Laboratory for Electronics, Inc.  
2030 Wright Avenue, Richmond, California

We have completed analysis of the particulate fragments in the less than 10  $\mu$  sieved fraction of sample HST-309. The analysis procedure used was the same as described in earlier reports.<sup>(1-3)</sup> The results of radiochemical analyses of the sized batches of radioactive particles having equivalent circular diameters larger than 2  $\mu$  are presented as Table I. Also included in Table I are the equivalent  $^{238}\text{PuO}_2$  spherical diameters for the size ranges and mid-ranges of these measurements. Radiochemical analysis was performed of the particles remaining on the slides (after the particle isolations were completed). This result, the total equivalent  $^{238}\text{PuO}_2$  mass of particles which have equivalent circular diameters less than 2  $\mu$ , is shown in Table I. The results of the hollow-star exposures for particles having equivalent  $^{238}\text{PuO}_2$  spherical diameters between 0.1 and 1.8  $\mu$  are included as Table II. The equivalent  $^{238}\text{PuO}_2$  mass of particles having spherical diameters less than 0.1  $\mu$  is calculated as follows:

$^{238}\text{PuO}_2$ in particles on the slides from which "most" particles with spherical diameters $>1.3 \mu$ were isolated.* (see Table I)	$1.60 \times 10^{-2} \mu\text{g}$
$^{238}\text{PuO}_2$ in particles with equivalent $^{238}\text{PuO}_2$ spherical diameters from 0.1 to 1.8 $\mu$ as determined by the hollow star technique.	$-2.6 \times 10^{-3} \mu\text{g}$
$^{238}\text{PuO}_2$ in particles with equivalent $^{238}\text{PuO}_2$ spherical diameters $<0.1 \mu$ .	$1.34 \times 10^{-2} \mu\text{g}$

1. Particle Analysis of Radioactive Fragments with Diameters  $<20 \mu$  from Impacted Sample 3, W. Holland, Tracerlab, a division of Laboratory for Electronics, for Sandia Corporation, September 16, 1968.
2. Particle Analysis of Radioactive Fragments with Diameters  $<20 \mu$  from Impacted Sample 5, W. Holland, Tracerlab, a division of Laboratory for Electronics, for Sandia Corporation, September 17, 1968.
3. Particle Analysis of Radioactive Fragments with Diameters  $<10 \mu$  from Impacted Sample 15, W. Holland, Tracerlab, a division of Laboratory for Electronics, for Sandia Corporation, October 23, 1968.

\*"Most" refers to the fact that not all particles in the 1.3 - 3  $\mu$  spherical diameter size range were isolated from the slides. It is shown in Table II that 40 particles in this size range (1.3 - 1.8  $\mu$ ) were found by the hollow star technique after the manual isolations were completed.

In Table III the values are presented which show the numerical size distribution of radioactive particles in the  $<10 \mu$  sieved fraction of sample HST-309. Table IV contains the mass percentages per size range for radioactive particles in the less than  $10 \mu$  sieved fraction of sample HST-309.

The mass percent and cumulative mass percent values listed in Table IV are used to calculate the percentages of the total impacted mass (including the cumulative percentages) which are listed in Table V. These values are combined with the Table VI values which were obtained from Dr. S. Abrahamson of Mound Laboratory and then plotted as Figure 1. From Figure 1 it is evident that 99.8% of the mass of microspheres which were impacted remains in particles with equivalent  $^{238}\text{PuO}_2$  spherical diameters greater than  $44 \mu$ . Also  $2.14 \times 10^{-3}\%$  of the mass is found in particles with spherical diameters less than  $0.1 \mu$ .

TABLE I RESULTS OF RADIOCHEMICAL ANALYSIS

Size Ranges ( $\mu$ )	Equivalent $^{238}\text{PuO}_2$ Spherical Diameters Midranges ( $\mu$ )	Equivalent Circular Diameter Size Range ( $\mu$ )	Number of Particles per Size Range	Equivalent $^{238}\text{PuO}_2$ Mass per Size Range ( $\mu\text{g}$ )
$<1.3$	-	$<2.0$	-	$1.60 \times 10^{-2}$
1.3-3	1.4)	2-4	100	$1.5 \times 10^{-3}$
	1.6)	4-5	52	$1.2 \times 10^{-3}$
	1.7	5-7	34	$1.1 \times 10^{-3}$
	2.0)	7-9	10	$4.6 \times 10^{-4}$
3-5	4.1)	9-11	3	$1.2 \times 10^{-3}$
	4.0)	11-15	2	$7.7 \times 10^{-4}$

TABLE II NORMALIZED RESULTS OF MEASURING SAMPLE HST-309  
PARTICLES BY THE HOLLOW STAR TECHNIQUE

Size Range ( $\mu$ )	Equivalent $^{238}\text{PuO}_2$ Spherical Diameters	Midrange ( $\mu$ )	Number per Size Range	Equivalent $^{238}\text{PuO}_2$ Mass per Size Range ( $10^{-10}$ gm)
0.1 -0.14		0.12	$5.76 \times 10^3$	$6.0 \times 10^{-1}$
0.14-0.21		0.18	$2.56 \times 10^3$	$9.0 \times 10^{-1}$
0.21-0.30		0.26	$3.52 \times 10^3$	3.7
0.30-0.42		0.36	$6.40 \times 10^2$	1.8
0.42-0.61		0.52	$4.40 \times 10^2$	3.7
0.61-0.88		0.74	$1 \times 10^2$	2.4
0.88-1.3		1.09	40	3.1
1.3-1.8		1.6	<u>40</u>	<u>9.8</u>
	Totals		$1.31 \times 10^4$	$2.60 \times 10^1$

TABLE III NUMERICAL PERCENTAGES PER SIZE RANGE FOR RADIOACTIVE PARTICLES IN THE LESS THAN  $10 \mu$  SIEVED FRACTION OF SAMPLE HST-309

Size Range ( $\mu$ )	Equivalent $^{238}\text{PuO}_2$ Spherical Diameters Midrange ( $\mu$ )	Equivalent Circular Diameter Size Range	No. of Particles per Size Range	Frequency Percent per Size Range	Cumulative Numerical Percent per Size Range
0.1 -0.14	0.12		$5.76 \times 10^3$	43.3	43.3
0.14-0.21	0.18		$2.56 \times 10^3$	19.2	62.5
0.21-0.30	0.26		$3.52 \times 10^3$	26.5	89.0
0.30-0.42	0.36		$6.40 \times 10^2$	4.8	93.8
0.42-0.61	0.52		$4.40 \times 10^2$	3.3	97.1
0.61-0.88	0.74		$1 \times 10^2$	0.8	97.9
0.88-1.3	1.09		40	0.3	98.2
1.3-3	1.6)		40 )		
	1.4)	2-4	$1 \times 10^2$ )		
	1.6) 1.7	4-5	52 ) 236	1.8	100.0
	1.8)	5-7	34 )		
	2.0)	7-9	10 )		
3-5	4.1) 4.0	9-11	3) 5		
	4.0)	11-15	2)	0.04	100.0
		Total	13,301		

TABLE IV MASS PERCENTAGES PER SIZE RANGE FOR RADIOACTIVE PARTICLES IN THE LESS THAN  $10 \mu$  SIEVED FRACTION OF SAMPLE HST-309

Size Ranges ( $\mu$ )	Equivalent $^{238}\text{PuO}_2$ Spherical Diameters	Midranges ( $\mu$ )	Mass per Size Range ( $10^{-10}$ g)	Mass Percent per Size Range	Cumulative Mass Percent per Size Range
<0.1	-	-	$1.3 \times 10^2$	59.6	59.6
0.1 -0.14	0.12	0.12	$6.0 \times 10^{-1}$	0.3	59.9
0.14-0.21	0.18	0.18	$9.0 \times 10^{-1}$	0.4	60.3
0.21-0.30	0.26	0.26	3.7	1.7	62.0
0.30-0.42	0.36	0.36	1.8	0.8	62.8
0.42-0.61	0.52	0.52	3.7	1.7	64.5
0.61-0.88	0.74	0.74	2.4	1.1	65.6
0.88-1.3	1.09	1.09	3.1	1.4	67.0
1.3-3	1.6) 1.4) 1.6) 1.8) 2.0)	1.7	9.8) 15 ) 12 )52 11 ) 4.6)	23.8	90.8
3-5	4.1) 4.0)	4.0	12 )20 7.7)	9.2	100.0
	Total		<u>218.2</u>		

TABLE V MASS PERCENTAGES OF MICROSPHERES IN THE  $<10 \mu$  SIEVED SIZE RANGE

Equivalent $^{238}\text{PuO}_2$ Spherical Diameter Size Ranges ( $\mu$ )	Mass Percent per Size Range	Cumulative		Basis - $3.6 \times 10^{-3}\%$ of Microspheres Impacted are in $<10 \mu$ Sieved Fraction
		Mass Percent per Size Range	Mass Percent per Size Range	
$>0.1$	59.6	59.6	$2.14 \times 10^{-3}$	$2.14 \times 10^{-3}$
0.1-0.14	0.3	59.9	$1.1 \times 10^{-5}$	$2.16 \times 10^{-3}$
0.14-0.21	0.4	60.3	$1.4 \times 10^{-5}$	$2.17 \times 10^{-3}$
0.21-0.30	1.7	62.0	$6.1 \times 10^{-6}$	$2.23 \times 10^{-3}$
0.30-0.42	0.8	62.8	$2.9 \times 10^{-5}$	$2.26 \times 10^{-3}$
0.42-0.61	1.7	64.5	$6.1 \times 10^{-5}$	$2.32 \times 10^{-3}$
0.61-0.88	1.1	65.6	$4.0 \times 10^{-5}$	$2.36 \times 10^{-3}$
0.88-1.3	1.4	67.0	$5.0 \times 10^{-5}$	$2.41 \times 10^{-3}$
1.3-3	23.8	90.8	$8.57 \times 10^{-4}$	$3.27 \times 10^{-3}$
3-5	9.2	100.0	$3.31 \times 10^{-4}$	$3.60 \times 10^{-3}$

TABLE VI RESULTS OF SIEVING MICROSPHERES IN SAMPLE HST-309

Sieved Size Range ( $\mu$ )	Mass Percent	Cumulative Percent
$<10$	$3.6 \times 10^{-3}$	$3.6 \times 10^{-3}$
10-20	$3.1 \times 10^{-3}$	$6.7 \times 10^{-3}$
20-44	$2.0 \times 10^{-1}$	$2.1 \times 10^{-1}$
$>44$	99.79	100.00

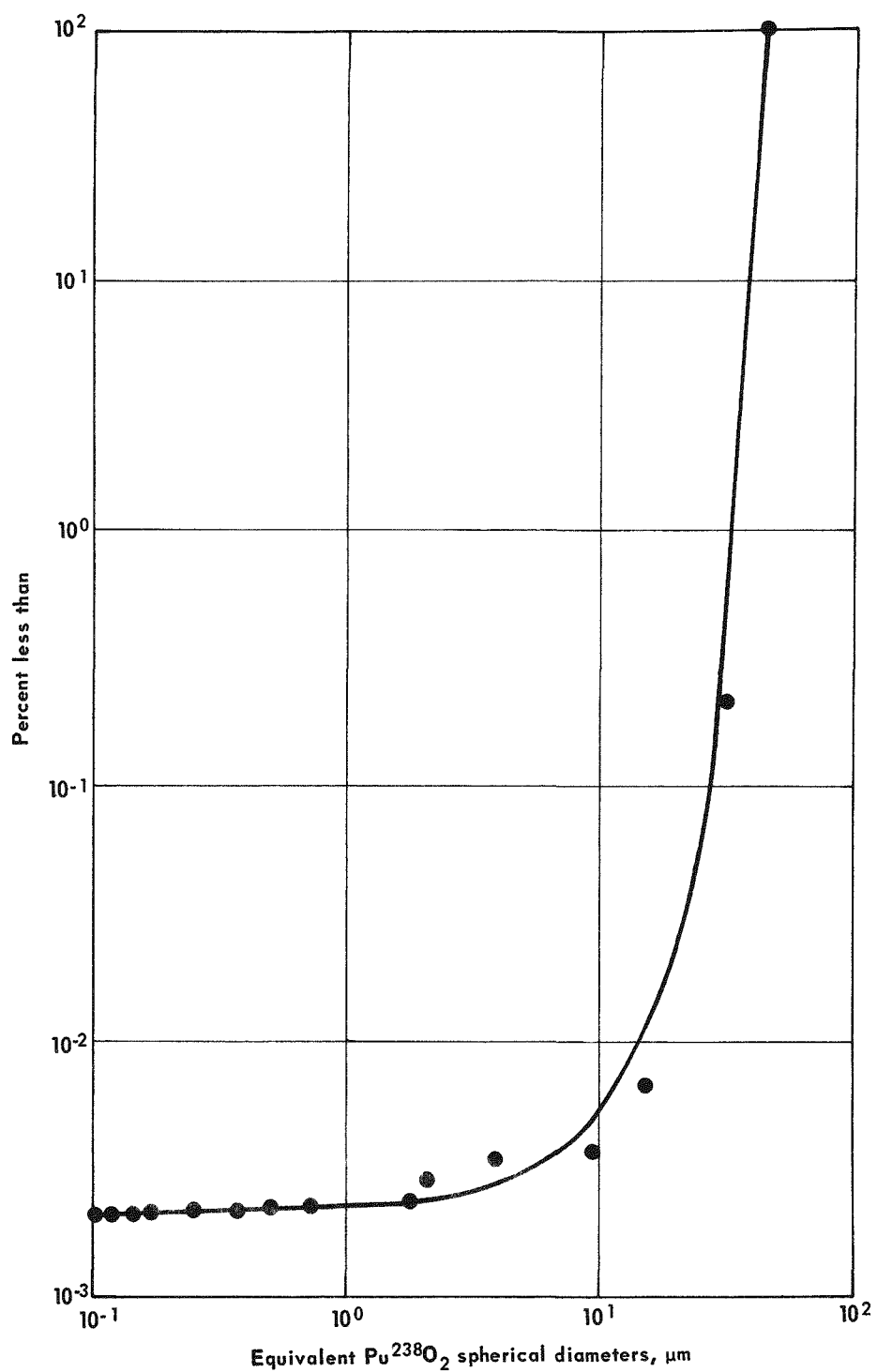


FIGURE 1 - Cumulative plot of mass percentages of all microspheres impacted in sample HST-309.

## APPENDIX E

### SUMMARY REPORT OF PLUTONIUM-238 PARTICULATE MATERIAL LESS THAN 10 $\mu$ IN SIZE AS REMOVED FROM FREE-FLOWING FUEL CONTAINED IN CAPSULE 361/368

Walter Holland, Tracerlab

A Division of Laboratory for Electronics, Inc.  
2030 Wright Avenue, Richmond, California

We have completed analysis of the particulate fragments in the less than  $10 \mu$  sieved fraction of sample 19-2. The analysis procedure used was the same as described in earlier reports.<sup>(1-3)</sup> The results of radiochemical analyses of the sized batches of radioactive particles having equivalent circular diameters larger than  $2 \mu$  are presented as Table I. Also included in Table I are the equivalent  $^{238}\text{PuO}_2$  spherical diameters for the size ranges and mid-ranges of these measurements. The results of the hollow-star exposures for particles having equivalent  $^{238}\text{PuO}_2$  spherical diameters between  $0.1$  and  $1.8 \mu$  are included as Table II. The equivalent  $^{238}\text{PuO}_2$  mass of particles having spherical diameters less than  $0.1 \mu$  is calculated as follows:

$^{238}\text{PuO}_2$  in particles on the slides from which  $8.1 \times 10^{-2} \mu\text{g}$   $>2 \mu$  particles have been isolated (see Table I).

$^{238}\text{PuO}_2$  in particles with equivalent  $^{238}\text{PuO}_2$  spherical diameters from  $0.1$  to  $1.8 \mu$  (see Table II)

$^{238}\text{PuO}_2$  in particles with equivalent  $^{238}\text{PuO}_2$  spherical diameters  $<0.1 \mu$ .  $6.37 \times 10^{-2} \mu\text{g}$

In Table III the values are presented which show the numerical size distribution of radioactive particles in the  $<10 \mu$  sieved fraction of sample 19-2. Table IV contains the mass percentages per size range for radioactive particles in the less than  $10 \mu$  sieved fraction of sample 19-2.

The mass percent and cumulative mass percent values listed in Table IV are used to calculate the percentages of the total impacted mass (including the cumulative percentages) which are listed in Table V. These values are combined with the Table VI values which were obtained from Dr. S. Abrahamson of Mound Laboratory and then plotted as Figure 1. From Figure 1 it is evident that 99.2% of the mass of microspheres which were impacted remains in particles with equivalent  $^{238}\text{PuO}_2$  spherical diameters greater than  $44 \mu$ . Also  $2.3 \times 10^{-3}\%$  of the mass is found in particles with spherical diameters less than  $0.1 \mu$ .

1. Particle Analysis of Radioactive Fragments with Diameters  $<20 \mu$  from Impacted Sample 3, W. Holland, Tracerlab, a division of Laboratory for Electronics, for Sandia Corporation, September 16, 1968.
2. Particle Analysis of Radioactive Fragments with Diameters  $<20 \mu$  from Impacted Sample 5, W. Holland, Tracerlab, a division of Laboratory for Electronics, for Sandia Corporation, September 17, 1968.
3. Particle Analysis of Radioactive Fragments with Diameters  $<10 \mu$  from Impacted Sample 15, W. Holland, Tracerlab, a division of Laboratory for Electronics, for Sandia Corporation, October 23, 1968.

TABLE I RESULTS OF RADIOCHEMICAL ANALYSIS

Size Ranges ( $\mu$ )	Equivalent $^{238}\text{PuO}_2$ Spherical Diameters	Equivalent Circular Diameter Size Range ( $\mu$ )	Number of Particles per Size Range	Equivalent $^{238}\text{PuO}_2$ Mass per Size Range ( $\mu\text{g}$ )
-	-	<2.0	-	$8.1 \times 10^{-2}$
1.5-2.0	1.5) 2.0)	1.75 2.0	605 234	$1.16 \times 10^{-2}$ $1.07 \times 10^{-2}$
2.0-3.0	2.2) 2.5) 2.9)	2.5 2.5 2.9	60 22 8	$3.81 \times 10^{-3}$ $2.09 \times 10^{-3}$ $1.13 \times 10^{-3}$

TABLE II NORMALIZED RESULTS OF MEASURING SAMPLE 19-2 PARTICLES  
BY THE HOLLOW STAR TECHNIQUE

Size Range ( $\mu$ )	Equivalent $^{238}\text{PuO}_2$ Spherical Diameters	Midrange ( $\mu$ )	Number per Size Range	Equivalent $^{238}\text{PuO}_2$ Mass per Size Range ( $10^{-10}$ gm)
0.1-0.14		0.12	$1.31 \times 10^4$	1
0.14-0.21		0.18	$2.37 \times 10^4$	8
0.21-0.30		0.26	$1.70 \times 10^4$	18
0.30-0.42		0.36	$3.44 \times 10^3$	10
0.42-0.61		0.52	$1.48 \times 10^3$	12
0.61-0.88		0.74	$1.56 \times 10^3$	37
0.88-1.3		1.09	$9.2 \times 10^2$	72
1.3-1.8		1.6	$6.0 \times 10^1$ 61,260	$\frac{15}{173}$

TABLE III NUMERICAL PERCENTAGES PER SIZE RANGE FOR RADIOACTIVE PARTICLES IN THE LESS THAN 10  $\mu$  SIEVED FRACTION OF SAMPLE 19-2

Size Range ( $\mu$ )	Midrange ( $\mu$ )	Equivalent Spherical Diameters	Equivalent Circular Diameter Size Range	No. of Particles per Size Range	Frequency Percent per Size Range	Cumulative Numerical Percent per Size Range
0.1-0.14	0.12			$1.31 \times 10^4$	21.1	21.1
0.14-0.21	0.18			$2.37 \times 10^4$	38.1	59.2
0.21-0.30	0.26			$1.70 \times 10^4$	27.3	86.5
0.30-0.42	0.36			$3.44 \times 10^3$	5.5	92.0
0.42-0.61	0.52			$1.48 \times 10^3$	2.4	94.4
0.61-0.88	0.74			$1.56 \times 10^3$	2.5	96.9
0.88-1.3	1.09			$9.2 \times 10^2$	1.5	98.4
1.3-2.0	1.6) 1.5) 1.7 2.0)	2-4 4-6		$6.0 \times 10^1$ ) 605 ) 899 234 )	1.5	99.9
2.0-3.0	2.2) 2.5) 2.5 2.9)	6-8 8-10 10-13		60) 22) 90 8)	0.1	100.0
		Total		62,189		

TABLE IV MASS PERCENTAGES PER SIZE RANGE FOR RADIOACTIVE PARTICLES IN THE LESS THAN  $10 \mu$  SIEVED FRACTION OF SAMPLE 19-2

Size Ranges ( $\mu$ )	Equivalent $^{238}\text{PuO}_2$ Spherical Diameters Midranges ( $\mu$ )	Mass per Size Range ( $10^{-10}$ g)	Mass Percent per Size Range	Cumulative Mass Percent per Size Range
<0.1	0.05	637	57.8	57.8
0.1-0.14	0.12	1	0.1	57.9
0.14-0.21	0.18	8	0.7	58.6
0.21-0.30	0.26	18	1.6	60.2
0.30-0.42	0.36	10	0.9	61.1
0.42-0.61	0.52	12	1.1	62.2
0.61-0.88	0.74	37	3.4	65.6
0.88-1.3	1.09	72	6.5	72.1
1.3-2.0	1.7	238	21.6	93.7
2.0-3.0	2.5	70	6.3	100.0
		1,103		

TABLE V MASS PERCENTAGES OF MICROSPHERES IN THE  $<10 \mu$  SIEVED SIZE RANGE

Equivalent $^{238}\text{PuO}_2$ Spherical Diameter Size Ranges ( $\mu$ )	Mass Percent per Size Range	Cumulative Mass Percent per Size Range	Mass Percent per Size Range	Cumulative Percent Mass
<0.1	57.8	57.8	$2.3 \times 10^{-3}$	$2.3 \times 10^{-3}$
0.1-0.14	0.1	57.9	$4 \times 10^{-6}$	$2.32 \times 10^{-3}$
0.14-0.21	0.7	58.6	$2.8 \times 10^{-5}$	$2.34 \times 10^{-3}$
0.21-0.30	1.6	60.2	$6.4 \times 10^{-5}$	$2.41 \times 10^{-3}$
0.30-0.42	0.9	61.1	$3.6 \times 10^{-5}$	$2.44 \times 10^{-3}$
0.42-0.61	1.1	62.2	$4.4 \times 10^{-5}$	$2.49 \times 10^{-3}$
0.61-0.88	3.4	65.6	$1.4 \times 10^{-4}$	$2.62 \times 10^{-3}$
0.88-1.3	6.5	72.1	$2.6 \times 10^{-4}$	$2.88 \times 10^{-3}$
1.3-2.0	21.6	93.7	$8.6 \times 10^{-4}$	$3.75 \times 10^{-3}$
2.0-3.0	6.3	100.0	$2.5 \times 10^{-4}$	$4.0 \times 10^{-3}$

TABLE VI RESULTS OF SIEVING MICROSPHERES IN SAMPLE 19-2

Sieved Size Range ( $\mu$ )	Mass Percent	Cumulative Percent
<10	$4 \times 10^{-3}$	$4 \times 10^{-3}$
10-20	$6.3 \times 10^{-2}$	$6.7 \times 10^{-2}$
20-44	$7.29 \times 10^{-1}$	$7.96 \times 10^{-1}$
>44	99.204	100

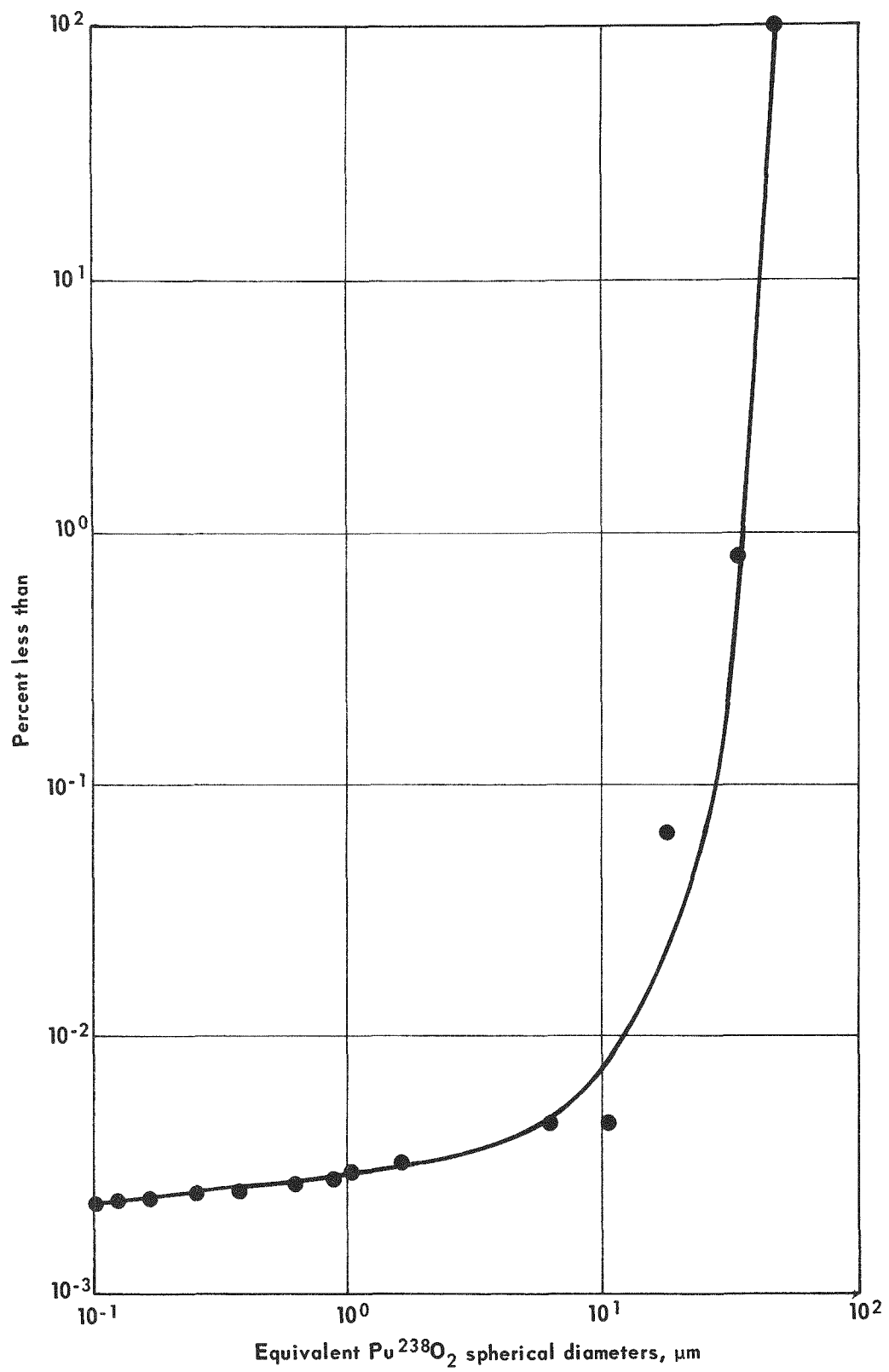


FIGURE 1 - Cumulative plot of mass percentages of all microspheres impacted in sample 19-2.